Advances in Air-Sea CO_2 Flux Measurement by Eddy Correlation

Byron W. Blomquist, Barry J. Huebert
Department of Oceanography, University of Hawaii, Honolulu, Hawaii, USA

Christopher W. Fairall, Ludovic Bariteau
Earth System Research Laboratory, NOAA, Boulder, Colorado, USA

James B. Edson
Department of Marine Sciences, University of Connecticut, Groton, Connecticut, USA

Jeffrey E. Hare
Joint Institute for Marine and Atmospheric Research, University of Hawaii, Honolulu, Hawaii, USA

Wade R. McGillis
Lamont Doherty Earth Observatory, Columbia University, Palisades, New York, USA

Aug 09, 2013

Abstract. Eddy correlation (EC) measurements of oceanic CO_2 flux are useful for the development and validation of air-sea gas exchange models and for analysis of the marine carbon cycle. Results from more than a decade of published work and from two recent field programs illustrate the principle interferences and demonstrate experimental approaches for improving measurement precision and accuracy. Water vapour cross-sensitivity is the greatest source of error for CO_2 flux measurements using infrared gas analysers (IRGA), often leading to a ten-fold bias in measured CO_2 flux. While various correction schemes have been demonstrated, the use of an air dryer and closed-path analyser is the most effective approach to eliminating this interference. This approach also obviates density or "Webb effect" corrections. Signal lag and frequency response are a concern with closed-path systems, but periodic gas pulses at the inlet tip provide for precise determination of lag time and frequency attenuation. Flux attenuation corrections are shown to be $< 5\,\%$ for a cavity ring-down analyser (CRDS) and dryer with a 60 m inlet line. The estimated flux detection limit for the CRDS analyser and dryer is a factor of ten better than for IRGA analysers measuring moist ambient air. While ship motion interference is apparent with all analysers tested in this study, decorrelation or regression methods are effective in removing most of this bias from IRGA measurements and may also be applicable to the CRDS.

Keywords: air-sea gas exchange, carbon dioxide, eddy correlation, flux measurement, infrared gas analyzer, cavity ring-down spectrometer

1. Introduction

Eddy correlation is a well established surface flux technique in carbon cycle research. Continuous flux observations are now routine across a global network of land-based sites (http://fluxnet.ornl.gov, Baldocchi et al., 2001), largely directed at determining net ecosystem exchange over seasonal timescales. The terrestrial research community has a clear focus on flux bias issues which potentially integrate to large errors in net ecosystem exchange, and a general consensus exists concerning standardised methods and data analysis procedures (e.g., Lee et al., 2004).

In contrast, the objectives of marine EC flux measurements are focused on short timescales of 15 minutes to an hour, where the the effects of physical forcing factors may be examined (McGillis et al., 2001a; Huebert et al., 2004; Marandino et al., 2007; Miller et al., 2010; Fairall et al., 2011). The principal motivation for air-sea flux measurements is development and validation of bulk flux and empirical gas transfer models for prognostic analysis of the ocean's role in energy budgets and biogeochemical cycles. The oceans are a net sink for carbon dioxide – roughly $2\,\mathrm{Pg\,C\,yr^{-1}}$ or one-third of the estimated annual anthropogenic production of CO_2 (Takahashi et al., 2002; Sabine et al., 2004; Jacobson et al., 2007; Takahashi et al., 2009). Global carbon cycle models are well developed, and in these models the air-sea CO_2 transfer coefficient, k_{co_2}, is often simulated by polynomial functions of the mean 10-meter wind speed ($\overline{u}_{10}$). A variety of quadratic and cubic wind speed dependencies have been proposed (Wanninkhof, 1992; Nightingale et al., 2000; Ho et al., 2006; Sweeney et al., 2007; Wanninkhof and McGillis, 1999; McGillis et al., 2001a; Prytherch et al., 2010b; Edson et al., 2011). In a study comparing the effects of quadratic and cubic representations, Takahashi et al. (2002) found a 70 % enhancement in both annual CO_2 uptake and wind speed sensitivity for the cubic k_{co_2} model. An uncertainty this large lends urgency to the task of identifying and quantifying the factors controlling air-sea gas exchange.

Contrasting experimental approaches for air-sea gas transfer studies have been developed: tracer studies utilising ambient gases (Rn, $^{14}CO_2$) or deliberately introduced tracers (^3He, SF_6) which integrate flux over timescales of a week or more (Wanninkhof, 1992; Nightingale et al., 2000; Ho et al., 2006; Sweeney et al., 2007; Ho et al., 2011), and direct EC flux measurements of CO_2 on hourly timescales (McGillis et al., 2001a; McGillis et al., 2004; Kondo and Tsukamoto, 2007; Weiss et al., 2007; Prytherch et al., 2010b; Miller et al., 2009; Miller et al., 2010; Lauvset et al., 2011; Edson et al., 2011). In general, EC measurements tend to support a cubic wind speed dependence for k_{co_2} while results

from tracer studies appear quadratic, although one long-term EC study at an inland-sea site with limited wind fetch also seems consistent with a quadratic model (Weiss et al., 2007). Solubility differences are surely one source of variability in k among the various gases, but a full explanation of the discrepancies remains elusive. There are large uncertainties associated with both experimental approaches. Improving EC measurement precision is therefore a high priority.

While the principles of EC flux measurements on land and sea are the same, marine studies present several unique problems. The oceanography community has yet to reach a consensus on methods to deal with all of these issues. Except in shallow coastal areas where fixed platforms are feasible, measurements must be made from a ship, drifting spar or moored buoy. Motion induced by waves and by changes in ship heading prevent a fixed coordinate frame of reference; high-rate wind measurements must therefore be corrected for platform tilt, rotation and velocity. Inevitable air-flow distortion caused by the ship's superstructure should be minimised and mean wind speeds corrected for its effects. Equipment must function in a hostile environment of salt spray and sooty emissions, where opportunities for cleaning and servicing in-situ sensors are often limited by hazardous conditions. Perhaps most important, air-sea CO_2 fluxes are quite small, often less than 3 mmol m^{-2} d^{-1} (1.5×10^{-3} mg CO_2 m^2 s^{-1}), yielding a concentration standard deviation of at most few tenths of a ppm on a background concentration of $\approx$ 390 ppm. A small flux over the vast expanse of the ocean is nevertheless significant to the global carbon cycle. This places a premium on superior signal-to-noise performance and freedom from interferences.

Marine CO_2 flux measurements have been done for at least 15 years. Several studies reporting ship-based EC measurements of CO_2 flux are listed in Table I. Flux measurements with closed-path infrared gas analysers (CP-IRGA) on early cruises (e.g. GasEx-98 and -01) were largely successful, despite numerous measurement challenges. There are well known issues related to EC sampling uncertainty, flow distortion, spectral attenuation, and density or "Webb" effects (i.e. the Webb, Pearman, Leuning or WPL theory: Lee and Massman, 2011; Webb et al., 1980), many of which can be corrected during data processing or minimised by appropriate experimental design. However, early trials revealed an additional interference related to platform motion. Water vapour cross-sensitivity, inherent to the broadband IR method, contributes further uncertainty (Fairall et al., 2000; McGillis et al., 2001a). In general, the flux detection limit was unfavourable over much of the ocean surface, limiting gas exchange studies to areas where air-sea CO_2 disequilibruim is large ($|\Delta pCO_2| \approx 60$ ppm).

Table I. Recent ship-based eddy correlation CO_2 flux studies

Project	Location	CO_2 Analyser	References
GasEx-98	N. Atl.	LI6262	McGillis et al.(2001a; 2001b)
GasEx-01	Eq. Pacific	LI6262	McGillis et al. (2004)
Arkona Spar[a]	Baltic	LI7500	Weiss et al. (2007)
MR05-03	Eq. Indian	LI7500	Kondo and Tsukamoto (2007)
G.O. Sars	N. Atl.	LI7500[b]	Lauvset et al. (2011)
Polarfront	N. Atl.	LI7500	Prytherch et al. (2010b)
Knorr07	N. Atl.	LI7500[c]	Miller et al.(2009; 2010)
SO GasEx	S. Ocean	LI7500	Edson et al. (2011)
DYNAMO	Eq. Indian	LI7500/LI7200[d]	this report
TORERO	Eq. Pacific	CRDS[e]	this report

[a] spar buoy, shallow water, limited wind fetch
[b] shrouded to limit optical contamination
[c] LI7500 converted to closed-path, with dryer
[d] two LI7200, with and without dryers
[e] Picarro G1301-f, with dryer

Subsequent studies tended to prefer the open-path gas analyser configuration (OP-IRGA) due to inherent advantages in frequency response, power consumption and wind measurement synchronisation. To-date, the popular choice has been a commercial instrument commonly used in terrestrial flux studies, the LI7500 (LI-COR Biosciences, Lincoln, Nebraska, USA). Unfortunately, experience has shown the effects of optical contamination and water vapour cross-sensitivity are severe with this design and complex corrections are required (Kohsiek, 2000; Prytherch et al., 2010a; Edson et al., 2011). Much of the discrepancy between observed and expected flux reported by Kondo and Tsukamoto (2007) may stem from this interference. As a result, flux measurement accuracy and precision has not improved. A case can be made that early CP-IRGA measurements were superior, although Prytherch et al. (2010a) and Edson et al. (2011) demonstrate some success in correcting the OP-IRGA water cross-sensitivity in post-processing. Corrections, however, are an order of magnitude larger than the flux.

Miller et al. (2010) have used an OP-IRGA in a modified closed-path configuration with an air dryer, yielding substantial improvement in flux measurement precision. A smaller, weather-proof version of the CP-IRGA with a very short sample inlet tube is recently available (LI-COR model LI7200), as are fast, high-sensitivity closed-path trace gas analysers based on cavity-enhanced IR absorption and cavity ring-down

spectrometry. Clearly, technology is advancing and new instruments are gaining wide acceptance in the carbon cycle research community.

It is appropriate at this time to summarise what has been learned over the last decade of ship-based CO_2 flux studies, examine the latest technical innovations, and begin the discussion toward a set of recommended experimental and data analysis procedures for EC flux measurements at sea. Our objectives in this paper are to examine the relative performance of new analysers with respect to the established methods and discuss the most significant errors resulting from instrumental and meteorological causes, showing how they may be eliminated, minimised or at least identified and removed from the data set. Flux data from two recent field programs will be used as a basis for critical evaluation of new methods. We conclude with a set of recommendations which seem to offer the best flux measurement precision under typical conditions for ship-based deployments.

2. Instrumental Methods

Closed-path IRGA instruments were the first to be developed and deployed for EC flux measurements (e.g., Jones et al., 1978) and commercial versions have been available for many years (e.g. LI-COR models LI6262, LI7000 and more recently the LI7200). All of these measure H_2O simultaneously with CO_2. Compensation for zero-drift and cross-sensitivity (memory effects) in the IR detector are necessary, and a band-broadening correction is computed for CO_2 based on the measured H_2O mole fraction (see LI-COR Application Note 129). Newer versions of the CP-IRGA measure optical cell temperature and pressure, enabling a real-time computation of molar mixing ratio from the measured molar density concentration. Except for the LI7200, CP-IRGA are bench-scale laboratory instruments and must be located in a protected enclosure. The obvious disadvantages are frequency attenuation in sample line tubing (low pass filtering) and a time lag between the wind and gas concentration measurements. Both of these problems are mitigated by appropriate experimental design.

An open-path IRGA employs the same operational principles in a miniaturised, weather-proof form suited to installation on sampling towers for in-situ measurements. Several early designs were developed (Ohtaki and Matsui, 1982; Kohsiek, 1991; Auble and Meyers, 1992) but the LI-COR LI7500 is the OP-IRGA in widespread use at this time. However, with an open-path optical cell it is not possible to measure temperature and pressure in the sample volume with sufficient speed and accuracy for a high-precision computation of molar mixing ratio.

Open-path IRGA CO_2 concentrations are typically computed as molar or mass density with appropriate WPL corrections applied as necessary.

Motion-related interference is a problem for all IRGA analysers at sea. This effect may correlate with residual motion contamination in the vertical wind measurement, leading to error in the computed flux. Water vapour interference is perhaps the most significant problem. In theory, the LI-COR algorithm accounts for cross-sensitivity. The correction is not perfect, however, and for a situation of minuscule CO_2 flux in the presence of a large H_2O flux, imprecision inevitably leads to bias in the computed CO_2 concentration. Because the interference correlates with water vapour flux (and vertical wind), the resulting CO_2 cospectrum is often dominated by water vapour crosstalk, leading to as much as a factor-of-ten error in the computed CO_2 flux.

Advances in tuneable diode laser technology inevitably led to the development of "cavity-enhanced" spectroscopic methods suitable for trace gas flux studies at ppm and ppb levels. Cavity ring-down spectrometers (CRDS) were first developed more than 20 years ago (O'Keefe and Deacon, 1988) and analysers for a variety of trace gases and analytical applications are commercially available (Picarro Inc., Santa Clara, California, USA). A similar method based on direct absorbance – off-axis integrated cavity output spectroscopy (OA-ICOS) – is a more recent development (O'Keefe et al., 1999; Baer et al., 2002). As with CRDS, OA-ICOS analysers for a variety of gases are manufactured commercially (Los Gatos Research, Mountain View, California, USA).

With cavity-enhanced methods, pressure broadening of the absorption line leads to cross-sensitivity with other components in the gas mixture. Water vapour is once again the principal offender. A correction for line broadening is therefore necessary, and most analysers include a water measurement in addition to the specific gases of interest. Because these are bench-scale instruments requiring sample inlet tubes, the usual caveats with respect to time lag and spectral attenuation also apply. In both methods, cavity pressure and temperature are carefully controlled and mole fraction or mixing ratio concentration may be computed with high precision.

3. Experimental

CO_2 flux measurements were included on two recent field programs as part of an ongoing effort to develop and evaluate new methods. In this section we present a brief overview of the experimental conditions and cruise details relevant to the flux tests.

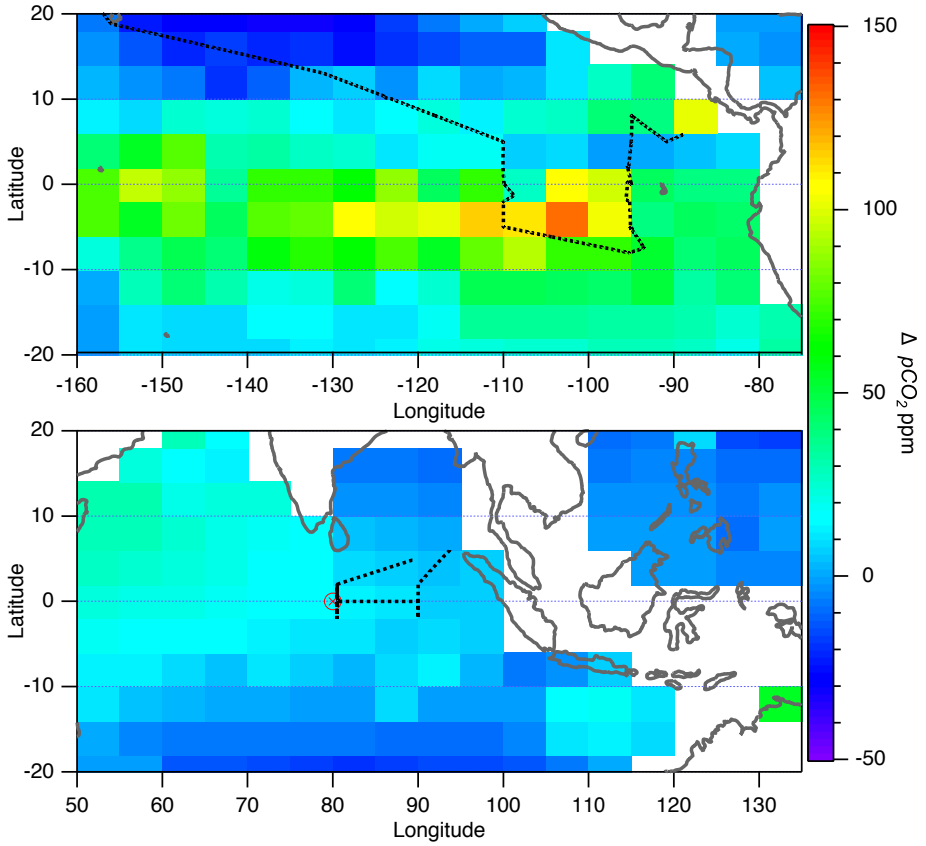

Figure 1. TORERO (Pacific Ocean) and DYNAMO (Indian Ocean) cruise tracks. ΔpCO_2 is plotted as the climatological mean for Nov–Dec (DYNAMO) and Jan–Feb (TORERO), from Takahashi et al. (2009). The DYNAMO study area is a weak source region for CO_2 with $\Delta pCO_2 \approx 30$ ppm. The TORERO cruise track transitioned from a weak sink area at 10° to 20°N into a very strong source region south of the equator in the East Pacific cold-tongue, where $\Delta pCO_2 > 100$ ppm.

3.1. DYNAMO

Project CINDY2011/DYNAMO (Cooperative Indian Ocean Experiment on Interseasonal Variability in Year 2011/Dynamics of the Madden-Julian Oscillation) was a multi-national, multi-platform investigation of ocean-atmosphere interaction in the Equatorial Indian Ocean. As one of three platforms providing DYNAMO surface observations, the ship R/V Roger Revelle occupied a station near 0°N, 80°E for the period August 2011 to February 2012, with periodic transits to Phuket, Thailand for resupply (see Figure 1). In this report we focus on Leg 3, from 07-Nov to 08-Dec-2011.

The NOAA/ESRL portable flux system (Fairall et al., 1997; Fairall et al., 2003) on the R/V Revelle recorded 10 Hz wind and motion measurements, bulk meteorological variables and sea surface temperature (SST). Three CO_2 IRGA analysers were installed in the following configurations: two LI7500 OP-IRGAs and one LI7200 CP-IRGA (University of Connecticut), mounted near the wind and motion sensors on the ship's forward mast; and one LI7200 (NOAA/ESRL) installed in a shipping container lab on the deck, drawing air from a teflon sampling tube extending up to the location of the mast flux sensors (30 m, 0.95 cm ID). Because the LI7200 differential pressure sensor has limited range, pressure drop considerations restricted the main sample line flow rate to $< 40\,\mathrm{L\,min^{-1}}$ STP for the lab installation. This analyser subsampled the high-flow inlet at $\approx 4\,\mathrm{L\,min^{-1}}$ STP and a pressure of ≈ 940 mb. A 200-tube Nafion air dryer (PD-200T-24-SS, Perma Pure LLC, Toms River, New Jersey, USA) was used with the lab analyser to reduce sample air dew point to $<-15\,^{\circ}\mathrm{C}$; water vapour band-broadening and dilution corrections for the lab LI7200 analyser were therefore negligible. The mast mounted LI7200 flow rate was $17\,\mathrm{L\,min^{-1}}$ through a 1 m by 0.95 cm ID inlet tube. Both LI7200 analysers record high-rate cell temperature and pressure for automated computation of dry CO_2 mole fraction. Optics for the LI7500 OP-IRGA were rinsed daily with distilled water to limit the effects of surface contamination.

A small equilibrator system and LI-COR 840 CO_2/H_2O analyser from Lamont-Doherty Earth Observatory was used to measure air-sea ΔpCO_2 from the ship's clean seawater supply. Measurements alternated between the atmospheric and equilibrator gas samples. A Nafion air dryer was used on the LI840 sample stream ($0.8\,\mathrm{L\,min^{-1}}$) to obtain dry-air concentrations.

Fluxes from the three IRGA analysers were computed from the standard "dry" mole fraction output of the LI7200 and the raw molar density output of the LI7500, with the latter corrected for dilution, WPL density perturbations and and vertical heave hydrostatic effects using a combination of fast and slow temperature and humidity measurements as in Edson et al. (2011) (see Section 6.1). Cospectra were computed from linearly detrended, motion corrected vertical wind velocity and fast CO_2 fluctuations in 10-minute segments. Filtering criteria for relative wind direction, ship manoeuvre parameters and reasonable limits on other variables such as motion correction variances were applied to select optimal measurement conditions: specifically, relative wind within 90° of the bow, heading standard deviation less than 5° and ship velocity standard deviation less than $1\,\mathrm{m\,s^{-1}}$. In addition, limits on $\partial CO_2/\partial t$, $\overline{u'co_2'}$ and $\overline{v'co_2'}$ were used to select for steady-state CO_2 conditions (see discussion in Section 6.5).

3.2. TORERO

Project TORERO (Tropical Ocean Troposphere Exchange of Reactive Halogen Species and Oxygenated VOC) was a multi-platform field program focussing on the distribution, reactivity and abundance of oxygenated organics and halogen radicals over the Eastern Pacific, from Costa Rica south to Chile. Surface observations on the NOAA ship R/V Ka'imimoana were performed from 10°N to 10°S along the 110°W and 95°W TAO buoy lines. The cruise covered the period 25-Jan-2012 to 27-Feb-2012, including transit from Honolulu, Hawaii at the start and to Costa Rica at the conclusion (see Figure 1).

A flux instrument package of wind and motion measurements equivalent to the DYNAMO system was installed on the R/V Ka'imimoana. Sensors were mounted at the top of a 10-meter meteorological tower on the ship's bow. Data acquisition hardware and a CRDS fast CO_2 analyser (Picarro model G1301-f) were located in the ship's instrumentation lab, ≈ 40 m aft of the bow tower. Compared to DYNAMO, sample inlet tubing was longer with more than double the flow: ≈ 60 m, 0.95 cm ID, and $80\,\mathrm{L\,min^{-1}}$ STP. Air pressure was ≈ 700 mb at the analyser inlet. Flow into the analyser was controlled at $\approx 5\,\mathrm{L\,min^{-1}}$ STP and, as in DYNAMO, an identical Nafion air dryer removed water vapour from the CO_2 sample stream. The CRDS analyser differs in one respect from a standard G1301 design with dual H_2O and CO_2 measurements; this spectrometer is configured to omit H_2O, devoting all measurement cycles to CO_2, yielding somewhat improved signal-to-noise performance (typically $\sigma_{co2} < 0.10$ ppm at 10 Hz).

Wind measurements (10 Hz) were corrected for motion interference using the Edson et al. (1998) method. Flux results were processed in 30-minute data segments with 10-minute overlap (i.e. four 30-minute segments per hour). The linear trend was subtracted from each data segment and a Hamming window applied to limit leakage of low frequency drift. Flux results were filtered with basic wind criteria: relative wind direction within 60° of the bow and standard deviation in relative wind direction <10° per 30-minute segment. Additional stationarity criteria and corrections for CRDS motion interference are discussed in sections 6.5 and 6.3 respectively.

4. Results: Flux Observations

4.1. DYNAMO: IRGA Analysers

During DYNAMO wind conditions were light and variable, punctuated by periodic wind events when the active phase of the Madden-Julian

Oscillation (MJO) was observed, starting on 24-Nov (Figure 2, upper panel). The atmospheric CO_2 concentration remained constant at $\approx$ 395 ppm with slight increases on 11-Nov and 23-Nov (Figure 2, lower panel). Leg 3 ΔpCO_2 was 20 ppm to 30 ppm, indicative of a weak source region for CO_2 (Figure 2, middle panel).

Because ΔpCO_2 for Leg 3 was positive and small, conditions were near the flux detection limit of the IRGA instruments, especially when winds were light. Throughout Leg 3 we expect a small, positive CO_2 flux. Figure 3 shows flux observed by the lab LI7200 is near zero or slightly positive, which confirms these expectations. This analyser shows a clear increase in CO_2 flux during strong winds on Nov 23-24 and Nov 28-29. In contrast, results from the mast LI7200 in the upper panel of Figure 3 show a much larger positive CO_2 flux, highly correlated to the water vapour flux ($\overline{w'q'}$, blue trace). The mast LI7500 sees a large negative CO_2 flux, anti-correlated to $\overline{w'q'}$. Mast measurements in Figure 3 incorporate WPL and dilution adjustments, and all IRGA CO_2 measurements include an internal LI-COR correction for water vapour crosstalk. Clearly, additional water vapour corrections are necessary for the analysers without dryers. Fluxes corrected with a cross-correlation procedure are shown in Figure 3 lower panel and discussed in Section 6.2.

A correlation between CO_2 mole fraction and air conditioner cycling was noted for the lab-mounted LI7200. Although this analyser is temperature compensated, we observe a clear residual sensitivity to room temperature fluctuations. Both analyser and sample line were insulated to damp this artefact. The air conditioner cycling frequency was sufficiently low that concentration drift related to room temperature variability should not contribute to flux over 10-minute integration times.

4.2. TORERO: CRDS Analyser

The TORERO cruise track transited a weak CO_2 sink region SE of Hawaii, eventually crossing a sharp boundary near the equator into the East Pacific cold-tongue upwelling, a persistent feature in pCO_2 climatology characterised by $\Delta pCO_2 >$ 100 ppm in Figure 1 (Takahashi et al., 2009). Wind speeds were in excess of 10 m s^{-1} during the transit from Hawaii, but slackened considerably near the equator and into the cold-tongue region.

CO_2 flux, wind speed and sea surface temperature are summarised in Figure 4. Seawater CO_2 measurements were not successful for this cruise due to instrument failure, but on the basis of January-February ΔpCO_2 climatology in Figure 1 we expect the initial portion of the

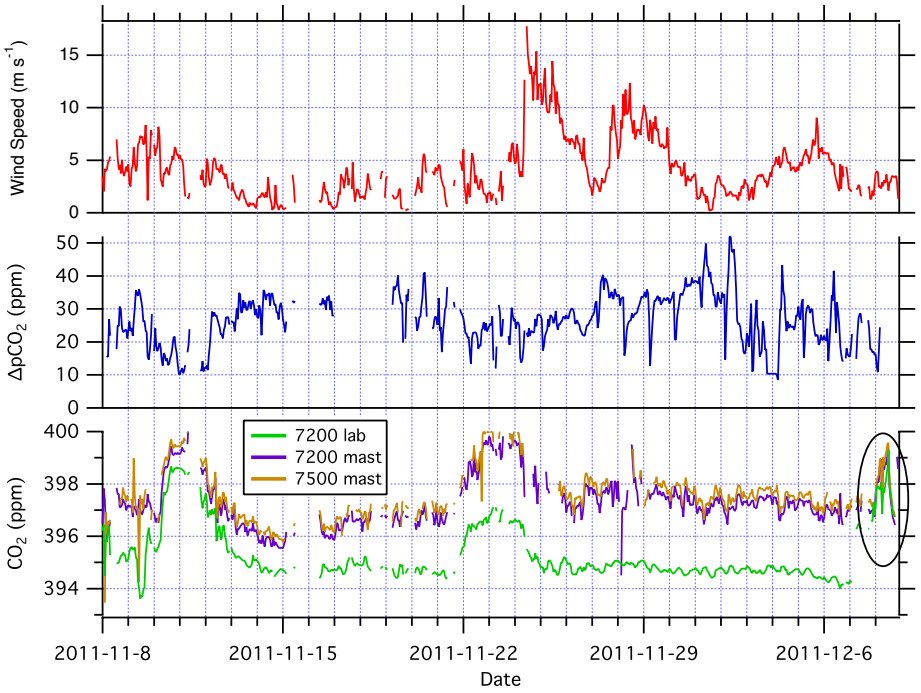

Figure 2. DYNAMO Leg 3: Time series of hourly mean wind speed, ΔpCO_2 and atmospheric dry CO_2 mixing ratio from three IRGA analysers. An offset of 2 ppm to 3 ppm is evident between the dry-air lab LI7200 measurement and mast mounted analysers. For the circled segment at the end of the leg, the Nafion dryer was removed from the lab LI7200 for a direct comparison with mast sensors. Without the dryer, the lab LI7200 "dry" molar mixing ratio output closely tracks the mast "dry" mole fraction measurements.

transit from Hawaii to be a weak sink region, with $\Delta pCO_2 \approx -20$ ppm to -30 ppm. The cold tongue region south of the equator should be a strong CO_2 source. Flux observations in Figure 4 confirm these expectations. The flux detection limit of the CRDS system is more than sufficient to reveal a negative flux across the weak sink region early in the cruise.

Estimating air-sea disequilibrium from the observed CO_2 flux is an interesting exercise and provides a sanity check on the quality of flux measurements. In Figure 5, ΔpCO_2 computed from the CRDS flux data and bulk flux model estimates of the transfer coefficient, k_{co2} from COAREG 3.0 (Fairall et al., 2011), compares favourably with January-February mean ΔpCO_2 from equatorial cruise data in the region from 95°W to 110°W (gridded SOCAT database: http://www.socat.info, Sabine et al., 2012). Trends in estimated TORERO ΔpCO_2 closely track the multi-year mean latitude gradient for this region.

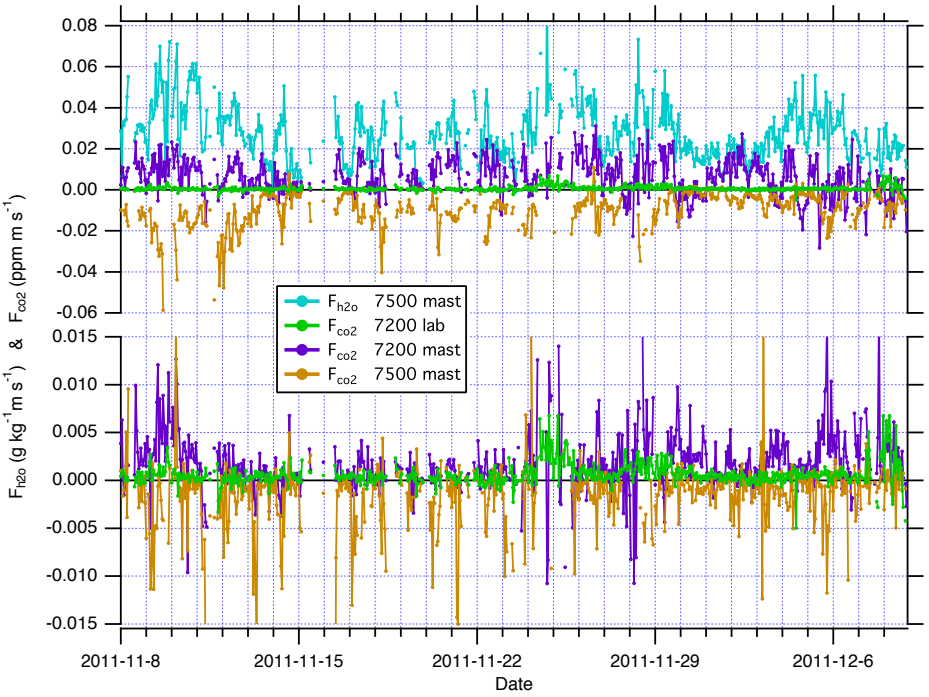

Figure 3. DYNAMO Leg 3: Time series of hourly F_{co2} ($\overline{w'co_2'}$) from the three IRGA analysers. The dry-air F_{co2} measurement from the lab LI7200 is plotted in green as a reference. In the upper panel, WPL and dilution corrected F_{co2} from mast analysers (purple and tan traces) roughly track F_{h2o} from the mast LI7500 ($\overline{w'q'}$, blue trace) and are about a factor of 14 greater than the lab LI7200 reference flux. Note, the mast LI7500 fluxes are negatively correlated to F_{h2o} while the mast LI7200 flux correlation is positive. The lower panel illustrates application of an additional water vapour cross-correlation correction to the mast analyzers (Edson et al., 2011) with $\Gamma_{7500} = 1.1$ and $\Gamma_{7200} = 0.93$ (see Section 6.2).

5. Results: CO_2 Analyser Performance

5.1. Noise Characteristics

Variance spectra for the CO_2 analysers are presented in Figure 6. CRDS background noise is "pink" with a characteristic slope of $\approx -1/2$. There is some indication of turbulent variance following a $-5/3$ power law at low frequencies in the mean TORERO spectrum which may be due to turbulent diffusion of horizontal atmospheric concentration gradients, but signal variance is largely dominated by sensor noise. CRDS noise (1σ) over the flux bandpass of 0.001 Hz to 5 Hz is 0.07 ppm.

Background noise in the IRGA analysers may also be "pink" based on the lab test spectrum for the LI7200 at constant CO_2 concentration, which is comparable to the CRDS result. However, LI7200 spectra

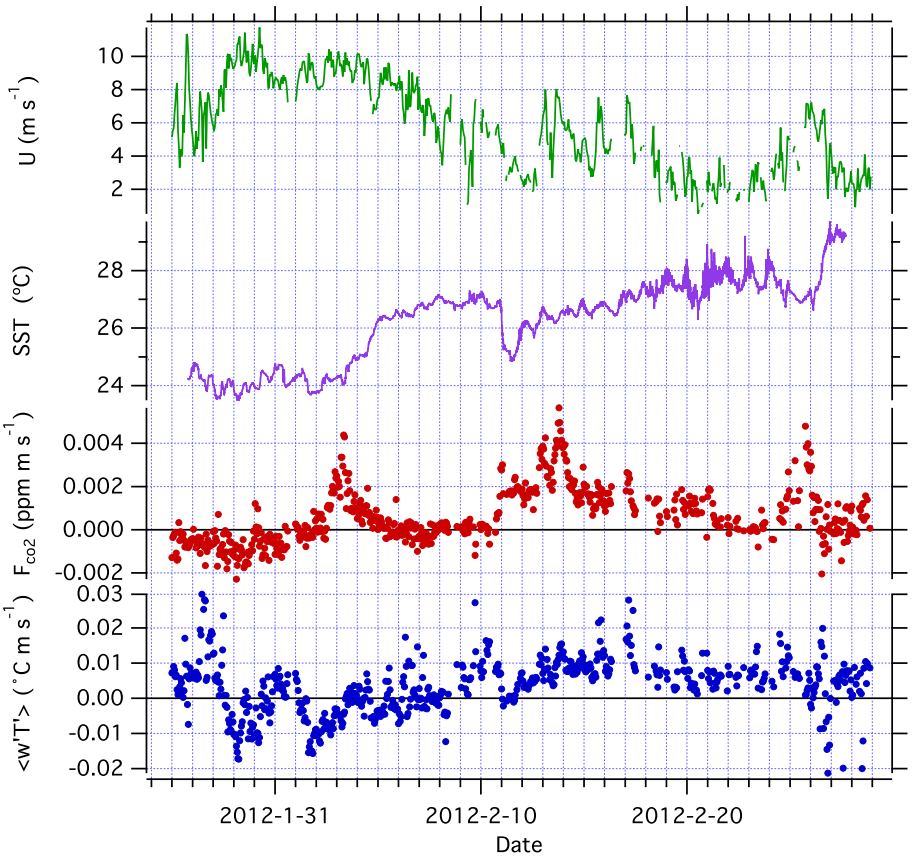

Figure 4. TORERO: hourly mean wind speed, SST, CO_2 flux and $\overline{w'T'}$. The transition to the E. Pacific cold tongue on 11-Feb is evident in the SST and F_{co2} measurements. Prior to 11-Feb, the transition from a weak CO_2 sink region through a fairly strong, localised source region and then to equilibrium conditions (27-Jan to 10-Feb) is apparent in the flux results. For the period when flux is near zero (5- to 10-Feb) $\sigma_{F_{co_2}} = 2.4 \times 10^{-4}$ ppm m/s. $\overline{w'T'}$ was generally less than 0.01 °C m s^{-1} throughout.

have an unexplained hump at 0.3 Hz to 0.6 Hz which is unrelated to water or motion interference and may arise from internal processing of the raw absorbances. This feature is not apparent in cospectra and therefore may not propagate into the flux measurement. A considerable fraction of IRGA CO_2 signal variance in moist air is due to water vapour crosstalk, illustrated by spectra of cross-correlation corrected CO_2 data (Figure 6, dashed lines).

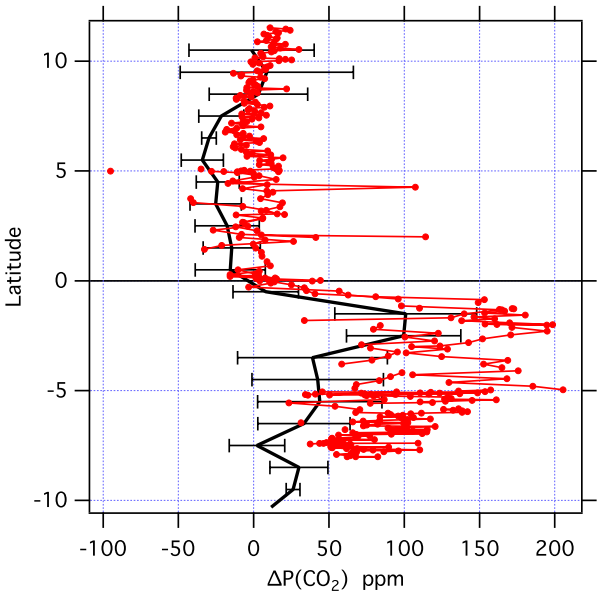

Figure 5. TORERO: ΔpCO_2 in the equatorial region of 95 °W and 110 °W. Red trace: estimated from observed F_{co_2} and computed k_{co_2} (COAREG 3.0, Fairall et al. 2011). Black trace: Jan-Feb mean for cruises along 95 °W and 110 °W from the gridded SOCAT database (Sabine et al., 2012). Error bars are 1σ.

5.2. Flux Detection Limit

To investigate the flux detection limit, we examine theoretical flux error as a function of air-sea disequilibrium (ΔpCO_2) and wind speed ($\overline{u}$). Flux error may be specified as a function of variance in both vertical wind (w) and scalar (CO_2) measurements, where CO_2 variance is composed of an atmospheric vertical turbulent flux component ($\sigma^2_{co_2\,a}$) and an "other noise variance" component ($\sigma^2_{co_2\,n}$, arising from analyser noise, water vapour crosstalk and other interferences), and where T is sampling time in seconds (after Fairall et al., 2000).

$$\delta F_{co_2} = \frac{2\,\sigma_w}{\sqrt{T}} \left[\sigma^2_{co_2\,a} \tau_{w\,co_2} + \sigma^2_{co_2\,n} \tau_{co_2\,n} \right]^{1/2} \tag{1}$$

The two terms in (1) are assumed to be independent, with characteristic integral time scales (τ). From the scatter in flux measurements under conditions where ΔpCO_2 is very low, and therefore $\sigma^2_{co_2\,a}$ is approximately zero, we can solve (1) for an empirical estimate of the "other noise" term.

$$\epsilon_n \equiv \sigma^2_{co_2\,n} \tau_{co_2\,n} \approx \left[\frac{\delta F^2_{co_2,0}\, T}{4\,\sigma^2_w} \right]_{\sigma^2_{co_2\,a} \approx 0} \tag{2}$$

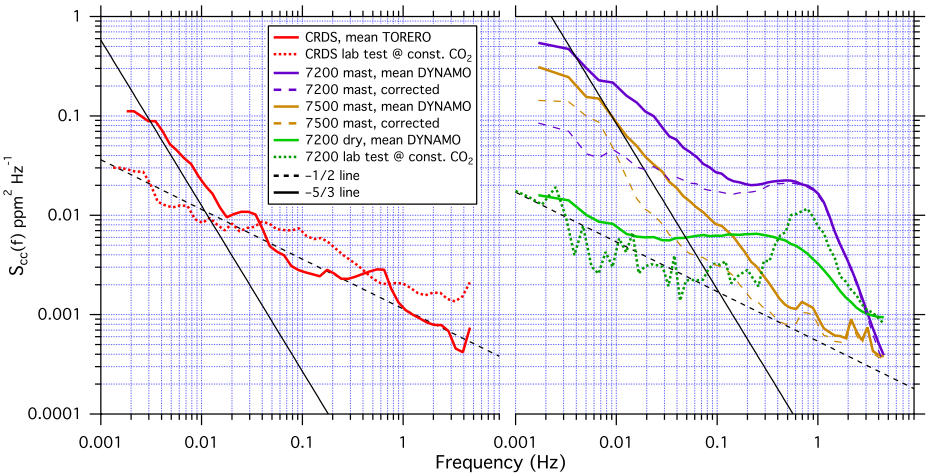

Figure 6. Mean variance spectra for the CO_2 analysers. Lab tests at constant CO_2 are shown as dotted lines. Left panel: CRDS spectra showing a characteristic "pink" noise background with a slope of $\approx -1/2$. The TORERO spectrum shows some indication of a -5/3 turbulence relationship at low frequencies, but is otherwise dominated by analyser noise. Right panel: IRGA spectra from DYNAMO, which also show a "pink" background noise characteristic. Application of the cross-correlation correction for water vapour interference (Edson et al., 2011) is shown as dashed lines. LI7200 spectra exhibit a broad hump of unknown origin peaking near 0.3 Hz to 0.6 Hz, noted in the raw LI7200 absorbance data for dry air DYNAMO measurements (green) and in the dry-air lab test (dotted green), so the effect is not related to water crosstalk or motion.

Quantities σ_w, $\sigma^2_{co_2\,a}$ and $\tau_{w\,co_2}$ in (1) are stability dependent. Monin-Obhukov similarity scaling may be used to express the stability dependence of variances through the following relationships,

$$\sigma_w = 1.25\, u_* f_w(z/L) \tag{3}$$

$$\sigma_{co_2\,a} = \frac{3\,F_{co_2}}{u_*}\, f_c(z/L) \tag{4}$$

$$\tau_{w\,co_2} = b\,\frac{z}{\overline{u_r}}\, f_\tau(z/L) \tag{5}$$

$$f_w(z/L) = (1 + 3\,|z/L|)^{1/3} \qquad (z/L < 0) \tag{6a}$$

$$f_w(z/L) = 1 + 0.2\,z/L \qquad (z/L > 0) \tag{6b}$$

$$f_{co_2}(z/L) = (1 + 20\,|z/L|)^{-1/3} \qquad (z/L < 0) \tag{7a}$$

$$f_{co_2}(z/L) = 1 + 1.0\,(z/L)^{1/2} \qquad (z/L > 0) \tag{7b}$$

$$f_\tau(z/L) = [\min(5,\, \max(0.5,\, (1 + 0.6z/L))]^{-1} \tag{8}$$

where L is the Obukhov length in meters and u_* is the friction velocity. In addition, an empirical relationship (5) may be used to specify the integral time scale, where $b = 2.8$ is a constant, and the functions f_w, f_{co_2} and f_τ are similarity relationships specifying stability dependence (unity for neutral conditions, see Blomquist et al., 2010).

Substitution of (3–8) into (1) yields an expression for flux error as a function of $\overline{u}$ and u_*, which can be further extended to the detection limit criterion, $\Delta pCO_2(u)$, by assuming an arbitrary error condition (e.g.$\approx \delta F/F = 1$, or 100% error), integration time (3600 seconds) and substitution of the standard bulk flux formulation, $F_{co_2}(u) = \alpha k(u) \Delta pCO_2$.

$$\Delta pCO_2 = \frac{2.50\, u_*\, f_w}{\alpha\, k\, \sqrt{3600}} \left[\left(\frac{3\, F_{co_2}\, f_{co_2}}{u_*} \right)^2 \frac{2.8\, z\, f_\tau}{\overline{u_r}} + \epsilon_n \right]^{1/2} \tag{9}$$

Here, $\overline{u}_r$ is mean relative wind speed (equivalent to $\overline{u}$ if the ship is not moving), α is dimensionless CO_2 solubility and k is the gas transfer coefficient. For this exercise, k, u_*, α and L were computed from the COAREG 3.0 bulk flux model (Fairall et al., 2011) with air temperature = 19 °C, SST = 20 °C, wind speeds from 1–16 m s^{-1} and default values for other inputs. Empirical values for the "other noise" term in (2) were determined for periods of near-zero CO_2 flux, yielding the following values (all as ppm^2 s): $\epsilon_{n,CRDS} = 0.00057$, $\epsilon_{n,7500} = 0.04574$, $\epsilon_{n,7200(dry,lab)} = 0.00867$ and $\epsilon_{n,7200(mast)} = 0.02043$. These values assume the best possible correction for water vapour interference in the mast-mounted sensors (see Section 6.2). We assume that ϵ is a constant, but for analysers with significant water vapour crosstalk the fraction of noise from that source may in fact have a wind speed dependence. Note that in (9), F_{co_2} is dependent on ΔpCO_2 and $\overline{u}$, so an iterative solution is necessary.

The detection limit criterion $\Delta pCO_2(u)$ computed from (9) for each analyser is shown in Figure 7a. The curves represent a theoretical lower limit on ΔpCO_2 for 100% error in the measured flux under slightly unstable, stationary conditions. $\Delta pCO_2(u)$ for error conditions other than $\delta F/F = 1$ scales inversely; for an error of $\delta F/F = 0.25$, the ΔpCO_2 criterion will be four times greater than indicated in Figure 7. We also note that, other things being equal, as SST decreases so does ambient ΔpCO_2 and therefore flux error will increase with decreasing SST. From Figure 7 it is clear analysers with a dryer perform considerably better than those without. This is also generally apparent in the scatter of flux measurements from Figures 3 and 4. The estimated detection limit for

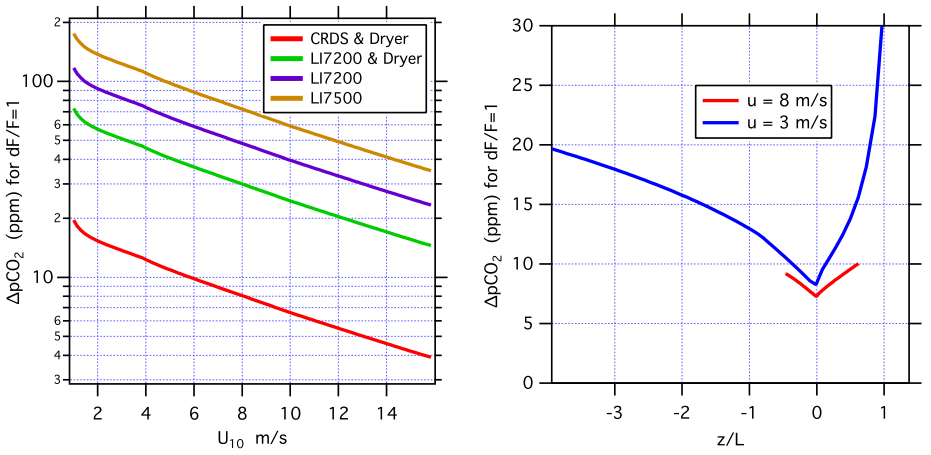

a. Detection Limits b. Stability Dependence

Figure 7. **a.** Flux detection limit criterion versus wind speed for each analyser, expressed as ΔpCO_2 ppm necessary for $\delta F/F$ =1 (i.e. 100 % error in observed F_{co_2} over 1 hr sampling time) under slightly unstable, stationary conditions. These results assume effective removal of water vapour cross talk bias in LI7500 and LI7200 analysers (see Section 6.2). **b.** Flux detection limit criterion for the CRDS analyser versus stability parameter z/L at low and moderate wind speeds. ΔpCO_2 computed from Equation (9). z/L and u_* obtained from the COARE 3.0 bulk flux model for two wind speeds with all input variables except air temperature held constant: T(air) = 8 °C to 16 °C, SST = 12 °C, RH = 80%, and u= 3 m s^{-1} or 8 m s^{-1}. Flux detection limit increases rapidly for stable conditions ($z/L > 0.5$) and light winds.

the dry-air CRDS measurement represents a factor-of-ten improvement over the earliest measurements with CP-IRGAs.

Figure 7b illustrates the CRDS detection limit as a function of the stability parameter z/L. In this case, k, L and u_* are obtained from COAREG model runs at two wind speeds (u = 3 and 8 m s^{-1}) under conditions where all bulk variables other than air temperature are held constant (T_{air} = 8–16°C, SST = 12 °C, RH = 80% and all other variables at default values). At a moderate wind speed of 8 m s^{-1}, the computed ΔpCO_2 criterion remains acceptable and the stability parameter has a narrow range about zero, even for large air-sea temperature gradients of ±4 °C. In light winds, however, z/L varies over a much wider range (blue trace) and the flux detection limit degrades rapidly under stable conditions when $z/L > 0.5$, or in this case when air temperature exceeds SST by more than 0.5 °C.

6. Results: Interferences and Corrections

Instrumental limitations, interferences, experimental constraints and meteorological conditions may all contribute to bias error in EC flux estimates. It is almost always necessary to apply corrections to computed cospectra or covariances to minimise these errors, usually at the expense of a (hopefully small) increase in random error. In this section we discuss the most significant sources of bias error and examine methods to avoid or correct for their effects.

6.1. Density Perturbations

Corrections to molar density fluxes for perturbations caused by heat and pressure fluxes are a well known issue with EC measurements (see review of WPL theory by Lee and Massman, 2011). For measurements on ships, Miller et al. (2010) have identified an additional pressure/density perturbation resulting from vertical heave. Other dynamic pressure effects are usually minor but may be important at higher wind speeds (Edson et al., 2008; Zhang et al., 2011). The sum of these interferences, if uncorrected, can lead to measurement bias greater than the actual ocean-atmosphere CO_2 flux. The OP-IRGA measurement is most affected by density fluctuations, requiring an accurate simultaneous determination of pressure fluctuations and sensible and latent heat fluxes. For the CP-IRGA, thermalisation in a long sample line eliminates the need for a sensible heat flux correction. Dynamic pressure effects are probably also less significant, but a fast pressure measurement may nevertheless be required for heave-related corrections unless analyser cell pressure is controlled to a constant value.

The fundamental assumption of WPL theory is a zero surface flux of dry air (Webb et al., 1980). The dry-air molar mixing ratio of a trace gas is a scalar quantity conserved in vertical motions and is therefore the preferred representation of concentration in conservation equations (Kowalski and Argueso, 2011). It is a considerable advantage if the analyser computes dry-air mixing ratio in real time from simultaneous measurements of CO_2, T, P and H_2O, eliminating the need for WPL corrections (Nakai et al., 2011). However, the accuracy of computed dry mole fraction is limited by calibration error and background noise in the T, P and H_2O measurements. Other things being equal, we expect the cavity-enhanced closed-path analysers, which control the optical cell to constant T and P, will yield better signal-to-noise than an analyser which relies on fast measurements of T and P for a real-time mole fraction calculation. Where possible, drying the air to a low, constant humidity should also be preferable to a computed water

correction if frequency attenuation effects of the dryer are not severe. The mean magnitude of WPL corrections to the DYNAMO LI7500 flux measurements was 35 %. For the mast-mounted LI7200 we rely on the real-time computation of mole fraction from measured T and P and WPL corrections are unnecessary.

6.2. Water Vapour Cross-Sensitivity

In addition to density effects, water vapour presents a direct interference to the CO_2 measurement in IRGA and cavity-enhanced instruments. The effect is illustrated by lab test results shown in Figure 8. Here the LI7200 and Picarro CRDS analysers drew air from a common gas sample manifold. Dry air from a compressed gas cylinder had a CO_2 concentration of 423 ppm and negligible water vapour. Upon humidification to a specific humidity of $\approx 11\,\mathrm{g\,kg^{-1}}$, the observed CRDS CO_2 concentration drops by more than 10 ppm as a result of line-broadening and dilution effects. The LI7200 mixing ratio, band broadening corrected in the analyser but not dilution corrected, dropped by 6.5 ppm. Application of the manufacturer's water vapour correction to the observed CRDS signal (Rella, 2010) yields a corrected mixing ratio very close to the original dry-air value, with a slight overcorrection bias of 0.1 ppm to 0.2 ppm. The computed LI7200 "dry" output (dashed green trace) yields an overcorrection bias of 1.1 ppm (0.24 %) which may arise from errors in the LI-COR band-broadening correction and/or error in the LI7200 H_2O calibration. Humidity was independently verified with a Vaisala HMP-35 T/RH sensor, so error in the band-broadening/cross sensitivity correction must explain most of the LI7200 bias.

The true CO_2 mixing ratio may be represented as the measured value minus a factor proportional to the specific humidity, q, where μ_0 is the proportionality or cross-correlation coefficient at zero frequency.

$$c = c_m - \mu_0 q \tag{10}$$

Assuming the 1.1 ppm overcorrection for the LI7200 in Figure 8 represents the water vapour crosstalk component in the CO_2 measurement, the cross-correlation coefficient at constant c and q is $\mu_0 = 1.1/11 = 0.10$ ppm kg $\mathrm{g^{-1}}$. Toward the end of DYNAMO Leg 3 the Nafion dryer was removed from the lab LI7200 for a direct comparison with the mast sensors (highlighted by the circled segment in Figure 2). Minus the dryer, computed LI7200 "dry" CO_2 mole fraction increases by $\approx$ 1.7 ppm. The change in q upon removing the dryer is about $17\,\mathrm{g\,kg^{-1}}$, yielding a second estimate for $\mu_0 = 0.10$, which is identical to the value observed in lab tests.

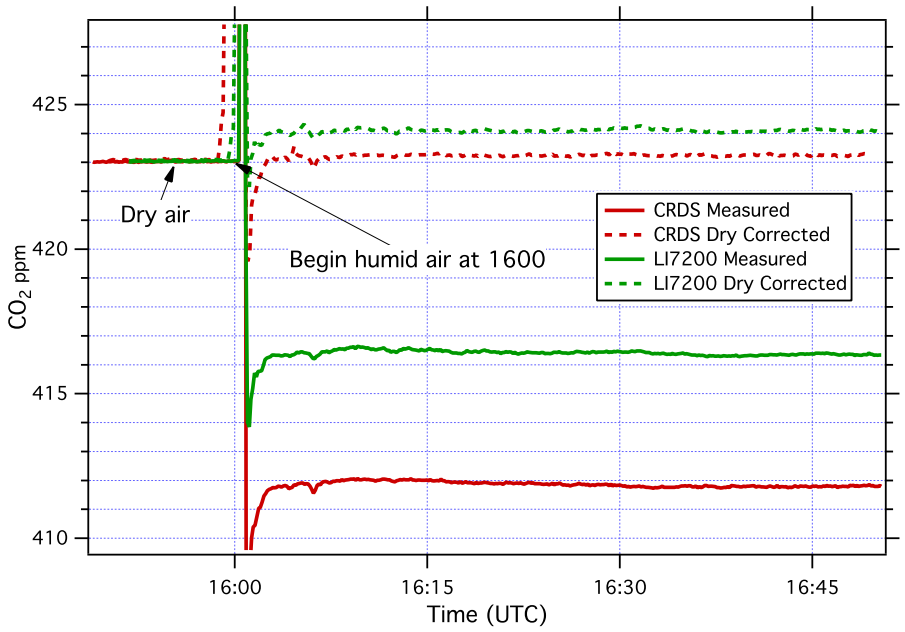

Figure 8. Laboratory test of CO_2–H_2O cross-sensitivity. Ten-second average data in dry air from a compressed gas cylinder. At 1600 UTC dry air flow was diverted through a Nafion humidifier, increasing dew point to $\approx 15\,^{\circ}\mathrm{C}$, or $\approx 11\,\mathrm{g\,kg^{-1}}$ specific humidity. The observed CRDS concentration, uncorrected for either line broadening or dilution, decreases by more than 10 ppm (red trace). The LI7200 wet mole fraction output, corrected for band broadening in the analyser but not for dilution, decreases by 6.5 ppm (green trace). Application of the manufacturer's recommended corrections for the CRDS (Rella, 2010) results in a slight over correction of ≈ 0.1 ppm (red dashed). The sum of dilution and band broadening corrections for the LI7200 yields a 1.1 ppm overcorrection compared to the dry-air value. (green dashed).

Equation (10) may be recast in flux terms (Equation A1, Edson et al., 2011).

$$\overline{w'c'} = \overline{w'c'_m} - \mu_0\,\overline{w'q'} \tag{11}$$

From (11) we therefore expect an error the in observed LI7200 CO_2 flux equal to 10 % of the water vapor flux ($\overline{w'q'}$). Mean DYNAMO latent heat flux of $100\,\mathrm{W\,m^{-2}}$ s at 29 °C and 1015 mb equates to $\overline{w'q'} \approx 0.0343\,\mathrm{g\,kg^{-1}\,m\,s^{-1}}$ and an expected CO_2 flux error of $\approx 3.43 \times 10^{-3}$ ppm m/s, or about 7.3 times the median dry-air LI7200 flux of 4.7×10^{-4} ppm m/s (Table II). Water vapour cross talk bias represented by μ_0 is therefore about half of observed error in moist air LI7200 CO_2 flux measurements from the mast, which are biased by a factor of 14 in Table II.

Figure 9 is an expanded view of CO_2 measurements for the period when the dryer was removed from the lab-mounted LI7200. In moist air, the computed "dry" mole fraction output of the lab LI7200

Table II. DYNAMO: median hourly F_{co_2} ($\pm 1\sigma$) for Leg 3. Flux computed as indicated in Section 3, despiked to remove extreme outliers. Results are shown for the base case (WPL and dilution corrections applied, where necessary) and two published water vapour cross-talk correction schemes.

		Median $F_{co_2} \pm 1\sigma$	(ppm m s^{-1})
	Base Case	PKT[a]	Cross-correlation[b]
LI7200 lab[c]	0.00047±0.00049	–	–
LI7200 mast[d]	0.00663±0.00396	0.00061±0.01423	0.00122±0.00155
LI7500 mast[e]	-0.00678±0.00314	-0.00254±0.00467	-0.00081±0.00222

[a] Prytherch et al. (2010a)
[b] Edson et al. (2011)
[c] dry-air data, WPL and dilution corrections not required
[d] computed from "dry" mole fraction output. No WPL/dilution correction
[e] WPL and dilution corrected

closely tracks the same output from the mast LI7200. In the published algorithm, LI-COR employs a function

$$\psi(m_w) = 1 + (a_w - 1)m_w \tag{12}$$

to obtain the corrected equivalent pressure of CO_2, where m_w is the mole fraction of water vapour and a_w is a constant specified as 1.15 for the LI7200 (see equation 3-16, LI-COR LI-7200 Manual, Publication No. 984-10564 and LI-COR Application Note 116). Recomputing the concentration from raw absorbances using published equations, with an adjustment of a_w =1.7, largely removes the offset observed in moist air (Figure 9, black trace). Similar results were obtained by doubling the LI7200 cross sensitivity factor, X_i, in equation 3-17 of the LI7200 manual. Bias in the computed dry mole fraction and excessive signal variance in moist air appears consistent across all three IRGA analysers, but these tests are insufficient to identify the specific source of the error in the LI-COR algorithm.

The correlation (or anti-correlation) between CO_2 and H_2O flux for the mast-mounted IRGA sensors in Figure 3 indicates considerable residual water vapour crosstalk in the "corrected" LI-COR CO_2 measurements. There may be a frequency dependency to the cross-correlation coefficient, μ, if, for example, the cross sensitivity term in the LI-COR algorithm has a frequency dependence or if hygroscopic behaviour of optical surface contaminants is involved. Thus, μ_0 obtained from lab tests at constant humidity will not represent the true flux error. In this case, the error cross-correlation coefficient may be

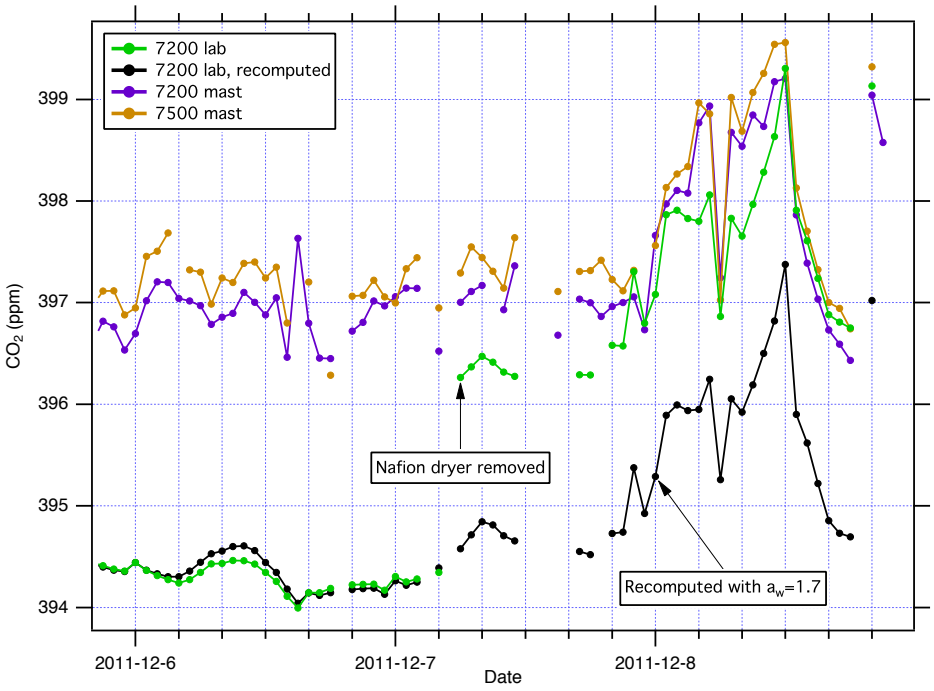

Figure 9. DYNAMO: CO_2 measurements for 6-Dec through 8-Dec. After 0400 UTC on 7-Dec, the Nafion air dryer was removed from the lab LI7200. From that point on, the dry mole fraction output of the lab LI7200 closely tracks dry mole fraction from the two mast-mounted IRGA analysers. Recomputing the lab LI7200 dry molar mixing ratio from raw absorbances (black trace) with an adjusted water crosstalk constant ($a_w = 1.7$ rather than 1.15) closely matches the analyser-computed result for the period with the dryer and does not show a bias following removal of the dryer. Adjusting the cross-sensitivity factor, X_i, produces a similar effect.

defined as

$$\mu = \frac{\int \mu(f) C_{wq}(f)}{\int C_{wq}(f)} \tag{13}$$

where $C_{wq}(f)$ is the $w'q'$ cospectrum and $\mu(f)$ is given by (Edson et al., 2011, equation 22) as

$$\mu(f) = \left(1 - \frac{C_{qc}(f)}{C_{qc_m}(f)}\right) \frac{C_{qc_m}(f)}{S_{qq}(f)} \approx \Gamma \frac{C_{qc_m}(f)}{S_{qq}(f)} \tag{14}$$

where Γ is an estimate for the term in parenthesis. For Γ, the difference from unity is a measure of the true atmospheric $q'c'$ cross-correlation and $\Gamma > 1$ indicates anti-correlation.

Related approaches have been developed to correct water vapour crosstalk and both are applied to the LI7200 and LI7500 mast-measured fluxes in this study. The PKT method (Prytherch et al., 2010a) is an

iterative correction applied to the raw time series to reduce the observed dependence of CO_2 on relative humidity. The cross-correlation method (Edson et al., 2011) is a spectral approach which seeks to preserve cospectral shape in the corrected result though a determination of $\mu(f)$ in (14). Application of the cross-correlation approach is complicated by the need to account for the real atmospheric component of $q'c'$ correlation. For SO-GasEx flux measurements, Edson et al. (2011) achieve best agreement with the PKT approach for $\Gamma = 0.88$, but in general we cannot expect Γ to be a constant. An analysis of water vapour correlation with a third, independent scalar measurement is one approach to obtain Γ, and Appendix A of Edson et al. (2011) illustrates the use of temperature fluctuations for this purpose. This approach was unsuccessful for DYNAMO, however, due to low sensible heat fluxes. In fact, temperature is not the best scalar for this purpose because $\overline{w'T'}$ approaches zero under near-neutral stability conditions prevalent at sea. An alternate scalar, such as dimethylsulfide, might prove more useful but was not available during DYNAMO. Lacking an independent estimate for the true atmospheric cross-correlation, mast-measured fluxes were scaled to the dry-air LI7200 flux. Best agreement between the mast-measured and dry-air CO_2 flux is obtained with $\Gamma_{7200} = 0.93$ and $\Gamma_{7500} = 1.1$ (project average values), indicating a real atmospheric $q'c'$ cross-correlation which is 7 % and 11 % of the measured $q'c'$ cross-correlation for these IRGA analysers during DYNAMO.

Cross-correlation corrected fluxes are plotted on the lower panel of Figure 3. Summary results for the PKT and cross-correlation approaches (median flux $\pm 1\sigma$) are provided in Table II. We find the PKT method yields some improvement in flux bias but leads to significantly increased variance in the final result. It is not possible to judge the accuracy of the cross-correlation correction since agreement with mean dry-air flux is the condition used to derive Γ, but the result is hopefully indicative of the improvement in both flux bias and variance that could result where an accurate and independent determination of Γ is available. Figure 10 shows project mean cospectra for the IRGA analysers and spectral effects of the cross-correlation correction. The water vapour crosstalk effect is observed at all frequencies across the flux measurement bandpass. Some distortion is apparent in the corrected cospectrum, but fluxes here are very small.

The source of IRGA water vapour crosstalk is often ascribed to hygroscopic contamination of optical surfaces. An analysis of the observed cross-correlation coefficient, $\mu_{obs} = \overline{q'c'_m}/\sigma_q^2$ (the first term in eq. A2, Edson et al. (2011)) provides a test of this hypothesis. If optical contamination is a major factor inducing cross-sensitivity, the magni-

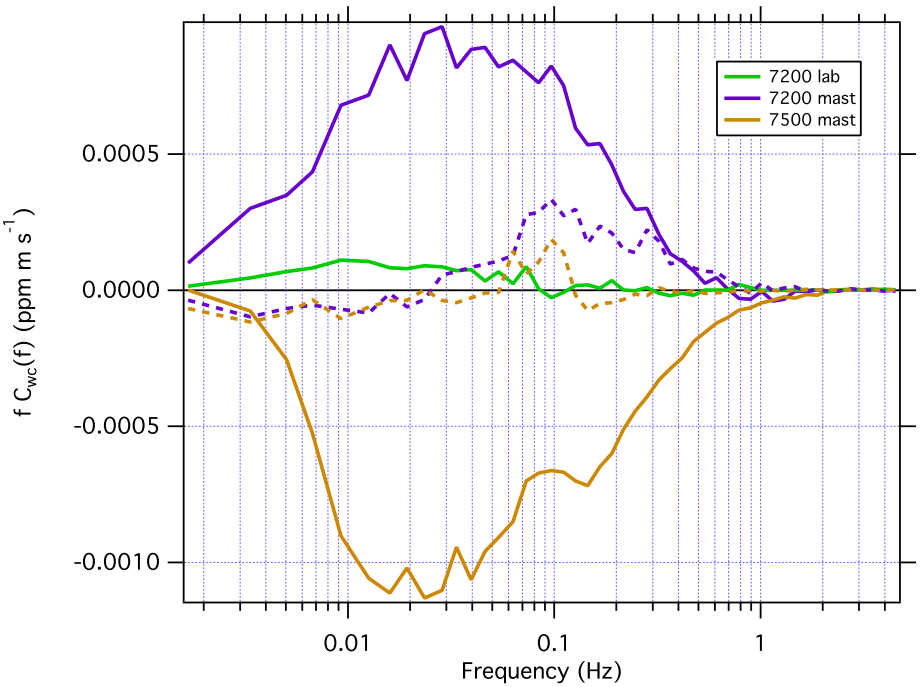

Figure 10. DYNAMO: Project mean cospectra for the IRGA analysers. Application of the cross-correlation correction for water vapour crosstalk as described in Section 6.2 (dashed lines) brings the mast IRGA cospectra closer to the dry-air LI7200 result. Spectral shape is distorted but fluxes are also very small.

tude of μ_{obs} should decrease significantly following a wash cycle on the LI7500 analyser. In fact, we find no significant shift in μ_{obs} when lenses are cleaned with distilled water; either optical contamination is not a source of $q'c'$ cross-correlation or (perhaps less likely) the relevant contaminants are resistant to removal by rinsing.

With respect to the use of an air dryer, laboratory tests with both the Picarro CRDS and LI7200 show the uncorrected CO_2 mole fraction remains constant following a large increase in water vapour. The Nafion dryer used in this work holds sample dew point to $<-15\,°C$ at flow rates up to $5\,L\,min^{-1}$ STP. At this level, water vapour effects are negligible and the bias noted in Figure 8 is absent. Use of a dryer was a major focus of the work reported in Miller et al. (2010) and these results confirm the basis of that approach.

6.3. Motion Related Effects for CO_2 Analysers

Motion interference is an issue unique to ship and aircraft flux measurements. For IRGA analysers, this effect was noted in the earliest field

studies but the exact cause remains uncertain. It may be due to modulation of the chopper wheel rotation (McGillis et al., 2001a) or flexing of the source filament (Miller et al., 2010). "Zero calibrations" with closed-path analysers (McGillis et al., 2001a; McGillis et al., 2001b) and shrouded "null" open-path sensors (Lauvset et al., 2011; Edson et al., 2011) have both been used as experimental approaches to quantify the ship-motion component of the measured flux, but computed corrections in data processing algorithms are more generally useful. Miller et al. (2010) employ a linear regression between observed CO_2 and the platform angular rates and linear accelerations to remove the motion-induced signal. For DYNAMO a motion decorrelation, mathematically equivalent to the linear regression approach and analogous to the moisture decorrelation described in Edson et al. (2011), was applied to raw CO_2 and H_2O data prior to subsequent water vapour corrections and flux computations. Motion influence is absent from cospectra in Figure 10, illustrating the effectiveness of the computed correction.

Motion interference with the CRDS analyser is apparent in cavity pressure spectra (Figure 11) and $w'co_2'$ cospectra (Figure 12), implying motion sensitivity in the pressure control system. Standard CRDS pressure control uses a single DC solenoid valve. In an attempt to reduce motion sensitivity, the manufacturer subsequently modified the analyser used in this study by installing two horizontally opposed valves. In theory, motion in one valve is offset by countervailing motion in the opposed valve. While the modification yields some improvement, TORERO results indicate it is only partially successful. In lab experiments, we find CO_2 sensitivity to variable cavity pressure is about $0.112\,\mathrm{ppm\ torr^{-1}}$. However, excess σ_{CO_2} due to motion (from the integrated area of the motion peak in the CO_2 spectrum) is about 2.5 times greater than expected given the observed σ_p at a sensitivity of $0.112\,\mathrm{ppm\ torr^{-1}}$, so additional factors are likely involved. As with the IRGA analysers, if motion response is roughly linear it may be possible to reduce or eliminate the interference with a regression or decorrelation approach.

For TORERO, motion interference in the CRDS CO_2 measurement was most significant during the outbound transit, when wind speeds were higher and the ship was making maximum headway into the wind and waves. Cospectra from the low-flux, high-motion transit leg and high-flux, low-motion equatorial portion of the cruise are shown in Figure 12. Motion interference is evident at 0.1 Hz to 0.3 Hz in the high-motion cospectrum. Flux is computed as the integral of the cospectrum, and for periods where motion interference was significant (707 of 2677 samples) a corrected flux estimate was obtained by fitting a baseline under the cospectral motion peak and eliminating it from

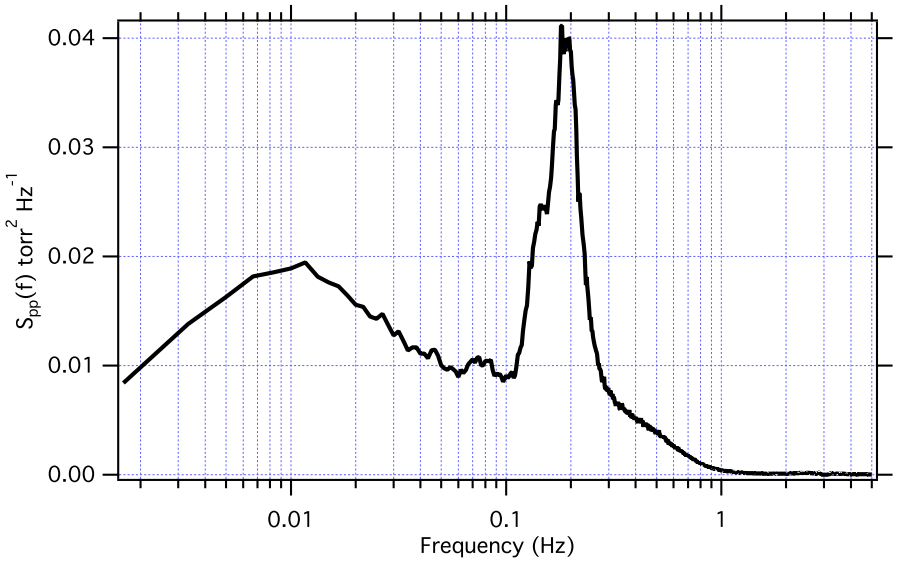

Figure 11. Mean CRDS cavity pressure spectrum for the first 100 hours of the TORERO cruise, when ship motion was greatest. Motion sensitivity of the pressure control system is apparent in the peak at 0.2 Hz.

the integral computation. The mean motion induced error for these flux measurements was 28 %.

One further source of error related to ship motion should be considered. We compute flux as the covariance of vertical wind and scalar measurements, $F_c = \overline{w'c'}$. Error in the wind motion correction leads to error in w', and vertical motion of the analyser or gas inlet through the CO_2 concentration gradient above the surface adds error to c'. If wind correction error is some fraction, f_m, of the computed motion, and motions are crudely sinusoidal, fractional error from these sources is shown to be (Blomquist et al., 2010)

$$\frac{\Delta F_c}{F_c} = \frac{f_m}{\kappa u_* \overline{z}} \frac{2\sigma_{w_m}^2}{\omega} \overline{\sin(\omega t)\cos(\omega t)} \tag{15}$$

where $\sigma_{w_m}^2$ is the variance of vertical motion of the sensor, $\kappa = 0.4$ is the Von Karman constant, $\overline{z}$ is mean measurement height and $\omega = 2\pi f$ is angular velocity of the motion.

Because the average of the product of sine and cosine is zero, we conclude motion and concentration terms are in quadrature and therefore do not contribute to flux. A peak at motion frequencies is, in fact, generally present in the quadrature spectrum, supporting this conclusion. However, assumptions of simple fractional dependence and sinusoidal motion are not exactly correct. For extreme high wind and

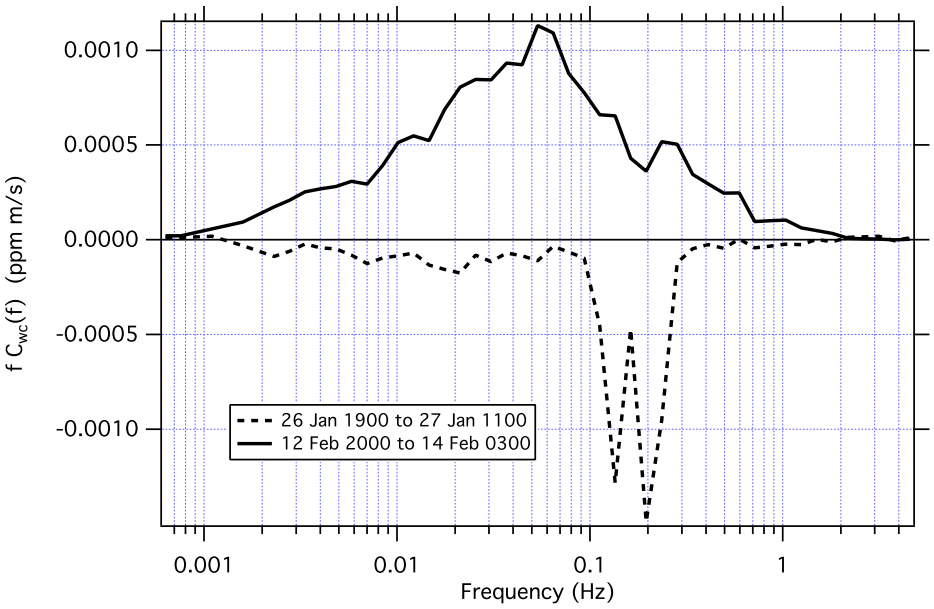

Figure 12. TORERO: CRDS cospectra for a 16-hour period early in the cruise with low negative F_{co_2} and high ship motion (dashed trace) and a 7-hour period of high positive F_{co_2} and low ship motion (solid trace). The motion effect is evident at 0.1 Hz to 0.3 Hz in the red trace. For the few measurements most affected by motion, a corrected estimate of the flux was obtained by fitting a baseline under the cospectral motion peak and removing it from the flux computation.

motion conditions ($f_m = 0.1\ \mathrm{s}^{-1}$, $\overline{u} = 20\ \mathrm{m\,s}^{-1}$, $u_* = 0.8\ \mathrm{m\,s}^{-1}$, $\omega = 0.6\ \mathrm{rad\,s}^{-1}$, $\overline{z} = 18$ m, and $\sigma^2_{w_m} = 6\ \mathrm{m}^2\,\mathrm{s}^{-2}$) the relationship reduces to the following (Blomquist et al., 2010).

$$\frac{\Delta F_c}{F_c} = 0.18\,(2\,\overline{\sin(\omega t)\cos(\omega t)}) \tag{16}$$

Thus, for the unlikely case that motion and concentration are in phase rather than in quadrature (i.e. $2\,\overline{\sin(\omega t)\cos(\omega t)} = 1$) and motion conditions are extreme, the worst case error is $\leq$18 %. This effect will contribute a slightly increased scatter to flux measurements in heavy seas.

6.4. Spectral Attenuation

All EC flux measurements are bandwidth limited and may therefore underestimate the true surface flux (see review by Massman and Clement, 2004). Resolution of the smallest eddies, at the highest frequencies, is primarily limited by sensor separation and sampling frequency, with additional low-pass filtering effects from tubing in closed-path systems.

Finite flux averaging periods and mean removal or detrending methods serve to high-pass filter the lowest frequencies. Over the ocean at moderate wind speeds, under near-stationary and sufficiently turbulent conditions, a thirty minute averaging period is usually sufficient to limit the loss of low-frequency flux signal. High frequency losses in closed-path systems are a more significant problem. Two general approaches have been used to deal with spectral attenuation corrections: transfer functions (Moore, 1986; Horst, 1997; Massman, 2000) and spectral similarity methods (Hicks and McMillen, 1988).

Flux is often computed as the integral of the observed cospectrum, which can be represented as the integral of the "true" cospectrum times a transfer function, $H(f)$ (e.g. as in Bariteau et al., 2010):.

$$F_{xm} = \int_0^{f_n} C_{wxm}(f)df = \int_0^{f_n} C_{wx}(f)\,[H(f)]^{1/2}df \tag{17}$$

where the subscript m refers to the measured quantity and f_n is the Nyquist frequency. For a closed-path CO_2 analyser subject to tube flow spectral attenuation (Lenschow and Raupach, 1991), $H(f)$ may be represented by a simple first-order low-pass filter process characterised by a time constant, τ_c:

$$H(f) = [1 + (2\pi f \tau_c)^2]^{-1} \tag{18}$$

Note that in (17), we use the square root of $H(f)$ because only the CO_2 signal is attenuated; w bandwidth is not considered a limiting factor. A model of the "true" cospectrum is required in (17). The normalised flat terrain, neutral-stability scalar cospectrum of Kaimal et al. (1972) is often used

$$\frac{fC_{wx}(f)}{F_x} = \frac{11n}{(1 + 13.3n)^{1.75}} \qquad n \leq 1.0 \tag{19a}$$

$$\frac{fC_{wx}(f)}{F_x} = \frac{4.4n}{(1 + 3.8n)^{2.4}} \qquad n \geq 1.0 \tag{19b}$$

where the surface normalised frequency $n = fz/\overline{u}_r$.

Given an estimate for τ_c, (18) and (19) may be used to derive an estimate of flux loss from high frequency spectral attenuation:

$$R_{attn}(z, \overline{u}_r) = \frac{\int_0^{f_n} C_{wx}(f)\,[H(f)]^{1/2}df}{\int_0^{f_n} C_{wx}(f)df} \tag{20}$$

A variety of methods can be used to obtain τ_c: 1) empirical experiments to characterise the transfer function of the inlet and analyser

system (e.g. Blomquist et al., 2010); 2) by invoking spectral similarity, the ratio of the attenuated cospectrum and a reference non-attenuated cospectrum, usually $C_{wT}(f)$, can be used to estimate the cutoff frequency, f_c – the point where the cospectral ratio drops by $1/\sqrt{2}$ from the unattenuated value – and then $\tau_c = 1/2\pi f_c$; or 3) a step impulse in CO_2 concentration can be introduced at the sample inlet tip. The resulting analyser response can be fit to a low-pass step response function (as in Peters et al., 2001)

$$s(t) = 1 \qquad t < t_{lag} \tag{21a}$$

$$s(t) = \pm \exp\left(\frac{t_{lag} - t}{\tau_c}\right) \quad t \geq t_{lag} \tag{21b}$$

where t_{lag} is the flow rate-dependent time delay of the inlet and the sign indicates whether the step is positive or negative.

The alternate approach to attenuation corrections via spectral similarity is useful when a simultaneous high-bandwidth scalar measurement is available for comparison. Sensible heat flux or $\overline{w'T'}$, as measured by the sonic anemometer, is often used for this purpose. Water vapour flux from an open path sensor (e.g. LI7500) is also suitable, and may be preferable when $\overline{w'T'}$ is near zero. The correction factor is computed by scaling the normalised attenuated scalar cospectrum to the normalised reference $w'T'$ cospectrum. Frequently, a subrange of unattenuated frequencies within the cospectrum is chosen as the basis for the scaling. Computation of the Ogives has also been employed as an expedient for similarity scaling in several recent reports of flux measurements with closed-path sensors (Spirig et al., 2005; Ammann et al., 2006; Miller et al., 2010). In addition to providing a basis for spectral attenuation corrections, the Ogive indicates if averaging time is sufficient to capture low frequency flux signal.

The Ogive is defined as the cumulative sum (integral) of the cospectrum (Oncley, 1989) from $f = 0$ to f_n and may be computed from a cospectrum averaged into n frequency bins on a log scale:

$$Og_{wx}(f_m) = \sum_{i=0}^{m} Co_{wx}(f_m)\Delta f_m \tag{22a}$$

$$m = 0, 1, 2, \ldots, n \tag{22b}$$

Normalised to total flux, and plotted together versus log frequency, the Ogive for the attenuated signal lies above the reference Ogive curve. The mean ratio of normalised Ogives,

$$R_{attn}(f) = \frac{Og_{wT}(f) \,/\, \overline{w'T'}}{Og_{wco_2}(f) \,/\, \overline{w'co_2'}} \tag{23}$$

over a range of frequencies where both measurements are assumed to be similar and unattenuated (typically 0.01 Hz to 0.1 Hz) is an estimate for the flux attenuation factor (Spirig et al., 2005; Ammann et al., 2006).

For the LI7200 and CRDS closed-path analysers in this study, a "puff" system was used to synchronise wind and CO_2 measurements, providing a convenient way to determine τ_c. A burst of nitrogen or compressed air from a solenoid valve, driven by a square-wave trigger with a period of 3 s to 5 s, is injected near the sample inlet tip at the beginning of each hour. The corresponding pulse in CO_2 response was matched to the recorded trigger pulse to determine inlet delay time. A low-pass response function (21) was fit to the rising (valve closure) edge of hourly pulses to determine τ_c. In this the case the second step response, when the valve closes, is judged a better representation of an ideal step impulse than the valve opening, which tends to overshoot due to the initial pressure surge. For TORERO, the mean time constant determined over 705 hours of measurements was $\tau_c = 0.126 \pm 0.008$ s ($f_c = 1.26$ Hz). Values were consistent over the entire project. Attenuation corrections computed from (20) and shown in Figure 13 represent a 5 % to 6 % correction when $\overline{u}_r = 12\,\mathrm{m\,s^{-1}}$ to $14\,\mathrm{m\,s^{-1}}$ and ≈ 1 % when $\overline{u}_r = 3\,\mathrm{m\,s^{-1}}$ to $5\,\mathrm{m\,s^{-1}}$. For DYNAMO, analysis of "puff" system response for the LI7200 lab analyser yields $t_{lag} = 6.2 \pm 0.2$ s and $\tau_c = 0.38 \pm 0.06$ s yielding a mean attenuation correction of ≈ 7 %.

Generally low sensible heat flux during TORERO limited the application of spectral similarity methods. As shown in Figure 4, $\overline{w'T'}$ observations were scattered about zero and generally smaller than $\pm$ $0.01\,^{\circ}\mathrm{C\,m\,s^{-1}}$. This is typical for the tropics, where sensible heat flux is much smaller than latent heat flux. Water vapour flux measurements were not available for TORERO. Figure 14 shows the ratio of normalised cospectra and Ogives for a period when both $\overline{w'T'}$ and $\overline{w'co_2'}$ yield reasonable cospectra. The Ogives cleanly approach the asymptote at both ends, indicating the measurement successfully captured turbulence frequencies contributing to the flux. The normalised Ogive curves are identical within the precision of the data, however, and it is difficult to determine an attenuation factor by scaling the two curves. From the cospectral ratio plot in Figure 14, it appears f_c should be near 1 Hz, but excessive noise again prevents a precise confirmation of τ_c by this method. Time constants from "puff" pulses over the same period yield an attenuation correction of ≈ 2.5 %. It is reasonable to expect some degree of spectral attenuation with the inlet tubing and dryer. For DYNAMO and TORERO, τ_c determined hourly from the step impulse response (as in Figure 13) is judged a more reliable measure of the attenuation correction. Attenuation is wind speed dependent, but even when $u > 15\,\mathrm{m\,s^{-1}}$ flux bias is less than 20 % so long as the inlet flow

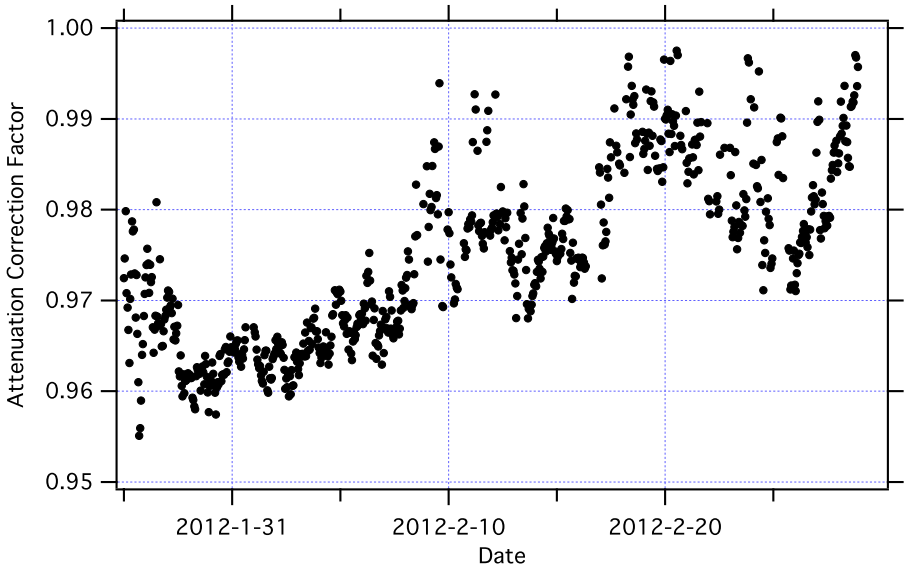

Figure 13. TORERO: Hourly frequency attenuation correction factors computed from the step impulse response to 3-second synchronisation "puffs". Observed flux is divided by the attenuation correction factor to account for the low-pass filtering effects of the inlet tubing, air dryer and analyser cavity volume. The correction is less than 4 % in almost all cases.

is fully turbulent. If the attenuation correction is precise to about the same degree, residual bias in the flux estimate will be less than 5 %.

We note that gases which adsorb or condense on tubing surfaces, such as water vapour, are the exception. Frequency attenuation can be much worse and variable, especially as tubing surfaces become coated with grime and hygroscopic contaminants (Leuning and Judd, 1996; Peters et al., 2001), which happens rapidly at sea. For this reason, open-path sensors are preferred for water vapour flux. EC measurements of soluble or reactive trace gases using long sample lines may also be problematic. Figure 15 shows the water vapour transfer function for the DYNAMO LI7200, plotted as the square root of the H_2O variance spectrum normalised to the LI7500, and as $\sqrt{H(f)}$ for $\tau_c = 0.55$ where

$$H(f) = [1 + (2\pi f \tau_c)^{1.3}]^{-1} \tag{24}$$

The degree of water vapour signal attenuation apparent in Figure 15 illustrates the significance of the problem, even for an analyser with a very short inlet tube and a high flow rate.

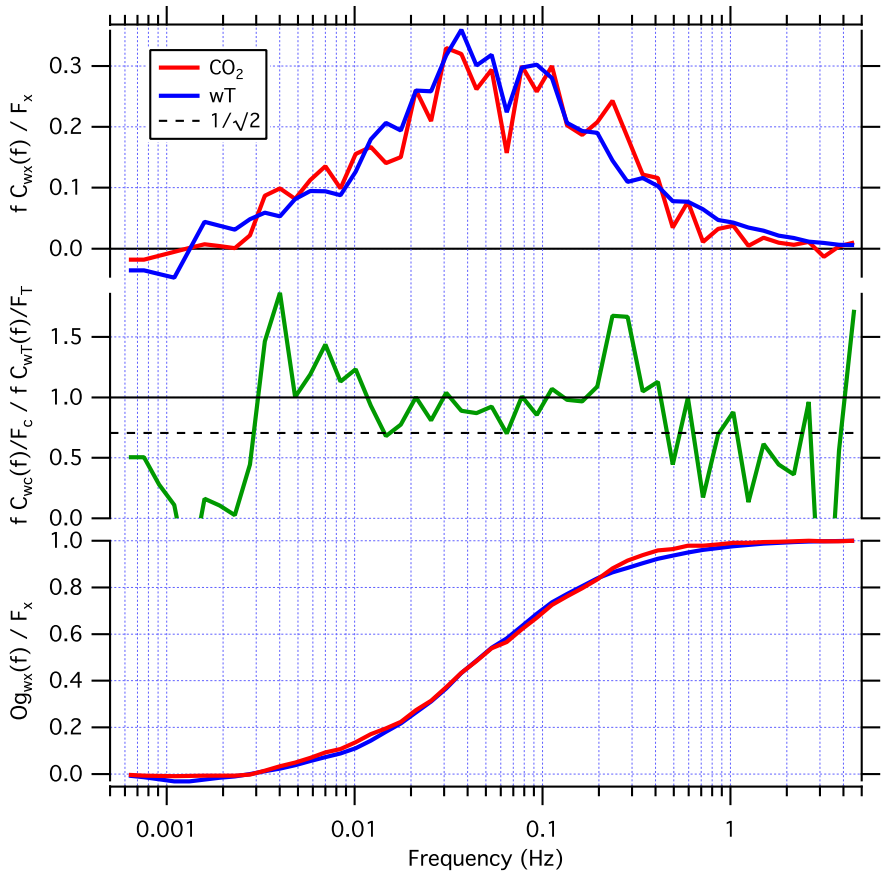

Figure 14. TORERO: Normalised $\overline{w'co_2'}$ and $\overline{w'T'}$ cospectra, cospectral ratio (green trace) and Ogives for 15-Feb, 1600–2300 UTC. This period is characterised by fairly large CO_2 and sensible heat fluxes with moderate winds ($\overline{u}_r = 9.3\,\mathrm{m\,s^{-1}}$, $\overline{u}_{true} = 6.2\,\mathrm{m\,s^{-1}}$). Nevertheless, noise prevents a clear determination of f_c from the cospectral ratio – the point where the ratio drops by $1/\sqrt{2}$, shown by the dotted line. Normalised Ogives for this period are identical within the precision of the data, again preventing precise determination of the small attenuation factor. Ogive curves approach the low frequency asymptote smoothly, indicating 30 minute integrations have adequately captured low frequency flux signal.

6.5. Stationarity, Homogeneity and Entrainment

While not an instrumental issue, evaluation of meteorological stationarity is an essential aspect of flux measurements. The use of theoretical cospectral models, such as Kaimal et al. (1972), and invocations of spectral similarity are only valid for steady-state conditions. In general, covariance flux at height z is only equal to the true surface flux under stationary, homogeneous conditions when there is no significant difference between entrainment flux at the marine boundary layer inversion

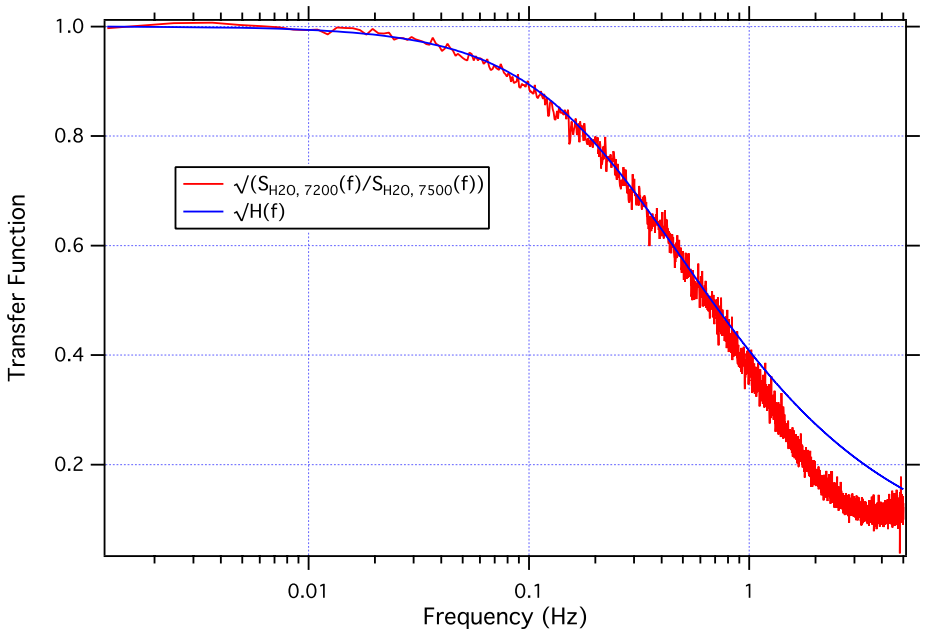

Figure 15. DYNAMO: Water vapour transfer function for the LI7200 following about one week of operation at sea. Further degradation in frequency response with time was observed over the course of the cruise leg. Red trace: square root of the 7200/7500 H_2O spectral ratio. Blue trace: transfer function derived from the best fit to equation (24). This result assumes the open path sensor is free of signal attenuation.

and surface flux (Businger, 1986). This is especially important in circumstances where surface fluxes are small and the magnitude of surface flux driven scalar variance is a minute fraction of the mean background concentration – Edson et al. (2008) provide a nice discussion of flux driven signal variance and mean concentration for DMS and CO_2, gases with greatly differing atmospheric lifetimes. Miller et al. (2010) report a large fraction of air-sea CO_2 flux measurements were discarded on the basis of stationarity criteria and Blomquist et al. (2012) show a similar sensitivity to stationarity issues in the measurement of air-sea carbon monoxide flux.

The evaluation of steady-state conditions tends to rely on somewhat subjective criteria. One widely used test for stationarity over the averaging interval is based on the fractional difference in covariance flux over 5- and 30-minute timescales (Gurjanov et al., 1986; Foken and Wichura, 1996; Lee et al., 2004). It is suggested that conditions are

stationary when the following ratio is less than 0.3,

$$RN_{cov} = \left| \frac{\overline{(\overline{w'x'})_5} - (\overline{w'x'})_{30}}{(\overline{w'x'})_{30}} \right| \leq 0.3 \tag{25}$$

where the numerator in (25) is the difference between the 30-minute covariance and the mean covariance from 5-minute sub-intervals of the same 30-minute data segment. In essence, this test asserts that for stationary conditions the flux fraction contributed by frequencies from ≈ 0.001 Hz to 0.007 Hz should be less than 30 % of the 30-minute covariance flux value. The true proportion of the flux signal expected at these frequencies is of course dependent on conditions. To be consistent, wind speed, measurement height and stability could be considered when specifying the length of the sub-interval or the fractional limit. In practice, the test in the form given above is routinely used as a rough filter for non-steady-state conditions.

Among TORERO 30-minute flux results passing relative wind and heading criteria ($N = 2352$) we find 165 observations exceed the 0.30 limit in (25). However, a few obvious outliers manage to pass the test – measurements where a single 30-minute value exceeds adjacent values by more than a factor of four – and many values near the flux detection limit are discarded which are not otherwise obviously bad. Figure 16 shows the time series of measurements over a 3-day period when CO_2 flux was essentially zero. Points in red fail the equation (25) test, presumably due to random low-frequency noise in measurements at or below the detection limit. Normally, it is desirable to retain these measurements.

Limiting the time-rate-of-change in the scalar variable ($\partial CO_2/\partial t$) is another test often used to screen for non-steady-state conditions. For DYNAMO and TORERO, the linear trend is removed from each flux data segment and the slope retained as a measure of $\partial CO_2/\partial t$. Here we extend this test by considering horizontal flux components $\overline{u'co_2'}$ and $\overline{v'co_2'}$. Figure 17 shows the distribution of horizontal flux with respect to $\partial CO_2/\partial t$ on TORERO for 2352 30-minute measurements passing relative wind direction criteria. Limits on $\overline{u'co_2'}$ and $\overline{v'co_2'}$ of ± 0.025 ppm m s^{-1} and on $\partial CO_2/\partial t$ of ± 0.5 ppm hr^{-1} were chosen to exclude extremes (shown as a bounding box in Figure 17) . Admittedly, these limits are also subjective. Applying this test, 72 of 2352 measurements are rejected, including almost all obvious outliers. Most results near the detection limit are retained. Flux measurements discarded by these criteria are illustrated in Figure 18 for a period of significant flux variability near the end of the TORERO cruise. For DYNAMO,

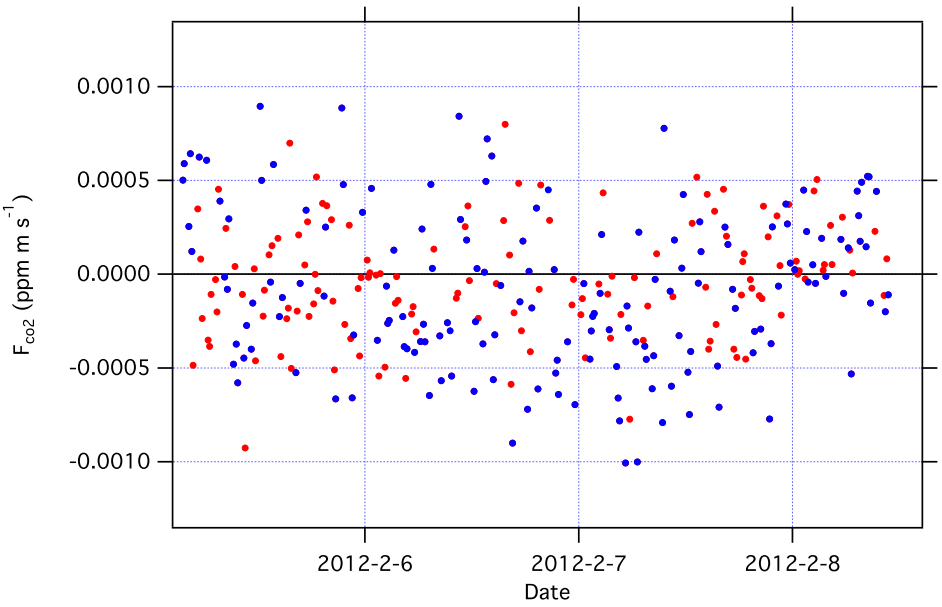

Figure 16. TORERO: CO_2 flux measurements from 5-Feb to 8-Feb-2012 (T =30 min), when measurements were uniformly distributed about zero. The covariance ratio stationarity test (Foken and Wichura, 1996) eliminates red data points. These observations are retained by alternate stationarity criteria illustrated in Figure 17.

similar limits were applied, removing 5 % of 10-minute dry-air flux measurements from the lab LI7200 which pass other basic criteria.

It should be noted the subjective limit on the magnitude of horizontal flux in this report (± 0.025 ppm m s^{-1}) is about ten times greater than the range in vertical flux values from Figure 4. Also, the limit of $\partial CO_2/\partial t < 0.5$ ppm hr^{-1} is a very small gradient; at $\overline{u}$ =8 m s^{-1} it represents an along-wind spatial gradient of about 1 ppm or 0.25 % of the mean background CO_2 concentration per 60 km. This implies weak spatial gradients in CO_2 can drive a signal variance from horizontal turbulent flux many times larger than CO_2 variance from surface flux alone. A similar situation has been reported for CO flux measurements at sea (Blomquist et al., 2012). Therefore, care should be exercised in choosing the location for field studies; areas affected by even moderate-to-low levels of continental pollution, for example, will provide fewer instances of suitable steady-state conditions, and a large fraction of measurements will be discarded.

Entrainment is an additional source of bias if a significant flux gradient develops between the ocean surface and marine boundary layer inversion. For CO_2, this may become a problem when pollution above the boundary layer subsides and is entrained. The situation is

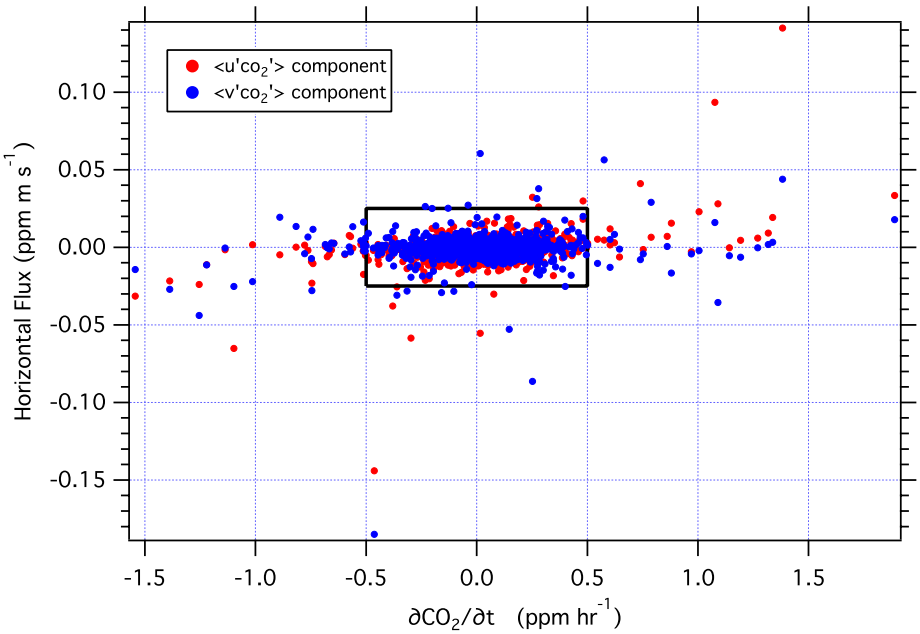

Figure 17. TORERO CO_2 steady-state criteria: $\overline{v'co_2'}$ (blue) and $\overline{u'co_2'}$ (red) turbulent fluxes versus $\partial CO_2/\partial t$ for 30-minute data segments. Flux measurements corresponding to points outside the black bounding box are excluded from the final hourly mean flux values. Note, limits to the magnitude of horizontal turbulent flux reflected by the bounding box are quite large (10x) compared to the range of vertical turbulent flux in Figures 4 or 18.

difficult to assess from surface measurements alone. Presumably, pollution entrainment leads to increased CO_2 variability, and appropriate stationarity criteria, as discussed above, serve to limit flux bias from entrainment.

7. Summary and Recommendations

This study provides further confirmation that water vapour interference is the most significant factor limiting precision and accuracy for ship-based CO_2 flux studies. These results are not definitive with respect to the cause of excessive water vapour crosstalk in the IRGA analysers, but the interference is apparent in both LI7500 and LI7200 models. Indeed, the LI7200, when used without a dryer, seems to offer few advantages over the LI7500 for air-sea CO_2 flux measurements. Computed CO_2 band broadening and dilution corrections in the LI-COR algorithm appear to be insufficiently precise for measurements of air-sea gas transfer and we cannot recommend CO_2 flux measurements in

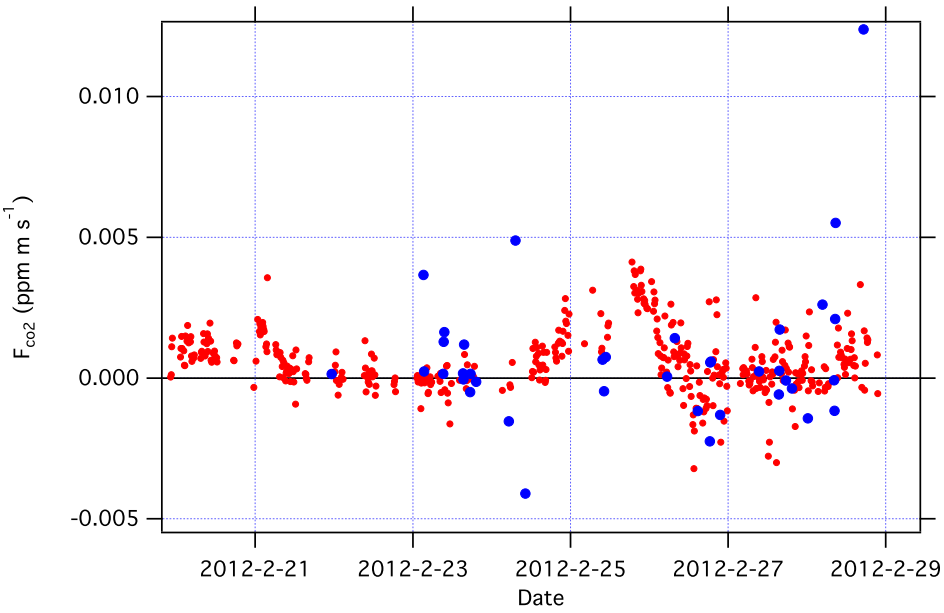

Figure 18. TORERO: CO_2 flux segment from late in the cruise illustrating instances where measurements were discarded (blue dots) on the basis of stationarity criteria in Figure 17.

moist air with the IRGA instruments. We were not able to test real-time water vapour corrections for the CRDS analyser due to the lack of an H_2O channel in our instrument. However, it is clear the dryer does not significantly compromise frequency response and there is much to be gained by eliminating water vapour crosstalk and WPL correction issues altogether, whichever analyser is used.

There may be conditions where space and power requirements of a closed-path analyser, large sampling pump and air dryer will present difficulties – on buoys, near-shore towers or for long-term unattended operation, for example. In this case there appears to be little recourse to the IRGA analyser. But complex corrections will be required (e.g. Prytherch et al., 2010a), measurement precision will be poor and a significant fraction of the observations may be discarded. Application of the cross-correlation correction scheme is facilitated by the measurement of a scalar other than temperature, free of water vapour interference, for an independent determination of the true $q'c'$ cross-correlation.

At high flow rates, long sample lines do not significantly degrade flux measurements with closed-path analysers. Where pressure drop at the analyser is a concern, empirical tests can determine the optimal trade-off between frequency attenuation and analyser performance. Cavity-enhanced analysers operate at low pressure and seem to tolerate

considerable pressure drop in the sample line, permitting high flow rates and adequate frequency response in almost all situations. A variety of useful methods exist to determine frequency attenuation and lag time. Hourly gas pulses at the sample inlet have proven most useful in our work, albeit at the expense of greater measurement system complexity. However, it seems worthwhile to verify attenuation corrections with spectral similarity methods when possible. Because sensible heat flux is often quite small, it is helpful to deploy the OP-IRGA for water vapour flux, if not for CO_2.

The issue of motion interference remains a concern for all CO_2 analysers studied to-date. While adjustments to cospectral shape can be used to correct motion artefacts, application of motion decorrelation or regression methods to the raw CO_2 time series is a fundamentally superior approach. These corrections have been demonstrated for IRGA analysers (Miller et al., 2010; Edson et al., 2011) and may also be applicable to the CRDS. In the future, analyser design modifications may reduce or eliminate this problem. We did not test an OA-ICOS cavity-enhanced analyser for this work. However, CO flux measurements at sea have been reported for this instrument under conditions of low to moderate ship motion, without significant interference (Blomquist et al., 2012).

Finally, we recommend a careful evaluation of scalar stationarity for flux measurements of CO_2 and other trace gases with long atmospheric lifetimes. Traditional stationarity tests are not always effective near the flux detection limit. An examination of horizontal turbulent fluxes can help improve selectivity of the stationarity test.

Acknowledgements

The authors gratefully acknowledge support from NSF grant AGS-1036062, the Office of Naval Research under Grant N00014-10-1-0546 and the NOAA Climate Program Office, Climate Observation Division. We are also grateful for the support and assistance of the officers and crew of the R/V Revelle and R/V Ka'imimoana.

References

Ammann, C., A. Brunner, C. Spirig, and A. Neftel: 2006, 'Technical note: Water vapor concentration and flux measurements with PTR-MS'. *Atmos Chem Phys* **6**, 4643–4651.

Auble, D. L. and T. P. Meyers: 1992, 'An open path, fast response infrared absorption gas analyzer for H_2O and CO_2'. *Boundary-Layer Meteorol* **59**, 243–256.

Baer, D. S., J. B. Paul, M. Gupta, and A. O'Keefe: 2002, 'Sensitive absorption measurements in the near-infrared region using off-axis integrated-cavity-output spectroscopy'. *Applied Phys B* **online only**, doi: 10.1007/s00340–002–0971–z.

Baldocchi, D., E. Falge, L. Gu, R. Olsen, D. Hollinger, S. Running, P. Anthoni, C. Bernhofer, K. Davis, R. Evans, J. Fuentes, A. Goldstein, G. Katul, B. Law, X. Lee, Y. Malhi, T. Meyers, W. Munger, W. Oechel, K. T. Paw U, K. Pilegaard, H. P. Schmid, R. Valentini, S. Verma, T. Vesala, K. Wilson, and S. Wofsy: 2001, 'FLUXNET: A new tool to study the temporal and spatial variability of ecosystem-scale carbon dioxide, water vapor, and energy flux densities'. *Bulletin Am Met Soc* **82**(11), 2415–2434.

Bariteau, L., D. Helmig, C. W. Fairall, J. E. Hare, J. Hueber, and E. K. Lang: 2010, 'Determination of oceanic ozone deposition by ship-borne eddy covariance measurements'. *Atmos Meas Tech* **3**, 441–455.

Blomquist, B. W., C. W. Fairall, B. J. Huebert, and S. T. Wilson: 2012, 'Direct measurement of the oceanic carbon monoxide flux by eddy correlation'. *Atmos Meas Tech* **5**, 3069–3075.

Blomquist, B. W., B. J. Huebert, C. W. Fairall, and I. C. Faloona: 2010, 'Determining the air-sea flux of dimethylsulfide by eddy correlation using mass spectroscopy'. *Atmos Meas Tech* **3**, 1–20.

Businger, J. A.: 1986, 'Evaluation of the accuracy with which dry deposition can be measured with current micrometeorological techniques'. *J Climate Appl Meteorol* **25**, 1100–1124.

Edson, J. B., M. D. DeGrandpre, N. Frew, and W. R. McGillis: 2008, 'Investigations of air-sea gas exchange in the CoOP coastal air-sea chemical flux program'. *Oceanography* **21**(4), 34–45.

Edson, J. B., C. W. Fairall, L. Bariteau, C. J. Zappa, A. Cifuentes-Lorenzen, W. R. McGillis, S. Pezoa, J. E. Hare, and D. Helmig: 2011, 'Direct covariance measurement of CO_2 gas transfer velocity during the 2008 Southern Ocean Gas Exchange Experiment: Wind speed dependency'. *J Geophys Res* **116**(C00F10), doi: 10.1029/2011JC007022.

Edson, J. B., A. A. Hinton, K. E. Prada, J. E. Hare, and C. W. Fairall: 1998, 'Direct covariance flux estimates from mobile platforms at sea'. *J Atmos Oceanic Technol* **15**, 547–562.

Fairall, C. W., E. F. Bradley, J. E. Hare, A. A. Grachev, and J. B. Edson: 2003, 'Bulk parameterization of air-sea fluxes: Updates and verification for the COARE algorithm'. *J Climate* **16**, 571–591.

Fairall, C. W., J. E. Hare, J. E. Edson, and W. McGillis: 2000, 'Parameterization and micrometeorological measurement of air-sea gas transfer'. *Boundary-Layer Meteorol* **96**, 63–105.

Fairall, C. W., A. B. White, J. B. Edson, and J. E. Hare: 1997, 'Integrated shipboard measurements of the marine boundary layer'. *J Atmos Oceanic Technol* **14**, 338–359.

Fairall, C. W., M. Yang, L. Bariteau, J. B. Edson, D. Helmig, W. R. McGillis, S. Pezoa, J. E. Hare, B. Huebert, and B. Blomquist: 2011, 'Implementation of the coupled-ocean-atmosphere respones experiment algorithm with CO_2, dimethyl sulfide, and O_3'. *J Geophys Res* **116**(C00F09), doi: 10.1029/2010JC006884.

Foken, T. and B. Wichura: 1996, 'Tools for quality assessment of surface-based flux measurements'. *Ag Forest Meteorol* **78**, 83–105.

Gurjanov, A. E., S. L. Zubkovskij, and M. M. Federov: 1986, ''Mnogokanalnaja avtomatizirovannaja sistema obrabotki signalov na baze". *EVM Geod Geophys Veroff* **R. II 26**, 17–20.

Hicks, B. B. and R. T. McMillen: 1988, 'On measurement of dry deposition using imperfect sensors and in non-ideal terrain'. *Boundary-Layer Meteorol* **42**, 79–84.

Ho, D. T., C. S. Law, M. J. Simth, P. Schlosser, M. Harvey, and P. Hill: 2006, 'Measurements of air-sea gas exchange at high wind speeds in the Southern Ocean: Implications for global parameterizations'. *Geophys Res Lett* **33**(L16611), doi:10.1029/2006GL026817.

Ho, D. T., R. Wanninkhof, P. Schlosser, D. S. Ullman, D. Hebert, and K. F. Sullivan: 2011, 'Toward a universal relationship between wind speed and gas exchange: Gas transfer velocities measured with $^3He/SF_6$ during the Southern Ocean Gas Exchange Experiment'. *J Geophys Res* **116**(C00F04), doi:10.1029/2010JC006854.

Horst, T. W.: 1997, 'A simple formula for attenuation of eddy fluxes measured with first-order-response scalar sensors'. *Boundary-Layer Meteorol* **82**, 219–233.

Huebert, B. J., B. W. Blomquist, J. E. Hare, C. W. Fairall, J. E. Johnson, and T. S. Bates: 2004, 'Measurement of the sea-air DMS flux and transfer velocity using eddy correlation'. *Geophys Res Lett* **31**(23).

Jacobson, A. R., S. E. M. Fletcher, N. Gruber, J. L. Sarmiento, and M. Gloor: 2007, 'A joint atmosphere-ocean inversion for surface fluxes of carbon dioxide: 1. Methods and global-scale fluxes'. *Global Biogeochem Cycles* **21**(GB1019), doi:10.1029/2005GB002556.

Jones, E. P., T. V. Ward, and H. H. Zwick: 1978, 'A fast response atmospheric CO_2 sensor for eddy correlation measurements'. *Atmos Environ* **12**, 845–851.

Kaimal, J. C., J. C. Wyngaard, Y. Izumi, and O. R. Cote: 1972, 'Spectral characteristics of surface-layer turbulence'. *Q J Royal Met Soc* **98**, 563–589.

Kohsiek, W.: 1991, 'Infrared H_2O/CO_2 sensor with fiber optics'. In: *Proceedings of the Seventh Symposium on Meteorological Observations and Instrumentation*. Amer Meteorol Soc, 14-18 January, New Orleans, LA, pp. 352–355.

Kohsiek, W.: 2000, 'Water vapor cross-sensitivity of open path H_2O/CO_2 sensors'. *J Atmos Oceanic Technol* **17**, 299–311.

Kondo, F. and O. Tsukamoto: 2007, 'Air-sea flux by eddy covariance technique in the Equatorial Indian Ocean'. *J Oceanography* **63**, 449–456.

Kowalski, A. S. and D. Argueso: 2011, 'Scalar arguments of the mathematical functions defining molecular and turbulent transport of heat and mass in compressible fluids'. *Tellus* **63B**, 1059–1066.

Lauvset, S. K., W. R. McGillis, L. Bariteau, C. W. Fairall, T. Johannessen, A. Olsen, and C. J. Zappa: 2011, 'Direct measurements of CO_2 flux in the Greenland Sea'. *Geophys Res Lett* **38**(L12603), doi:10.1029/2011GL047722.

Lee, X., W. Massman, and B. Law (eds.): 2004, *Handbook of micrometeorology: a guide for surface flux measurement and analysis*. Kluwer Academic Publishers.

Lee, X. and W. J. Massman: 2011, 'A perspective on thrity years of the Webb, Pearman, and Leuning density corrections'. *Boundary-Layer Meteorol* **139**, 37–59.

Lenschow, D. H. and M. R. Raupach: 1991, 'The attenuation of fluctuations in scalar concentrations through sampling tubes'. *J Geophys Res* **96**(D8), 15,259–15,268.

Leuning, R. and M. J. Judd: 1996, 'The relative merits of open- and closed-path analysers for measurement of eddy fluxes'. *Global Change Biol* **2**, 241–253.

Marandino, C. A., W. J. De Bruyn, S. D. Miller, and E. S. Saltzman: 2007, 'Eddy correlation measurements of the air/sea flux of dimethylsulfide over the North Pacific Ocean'. *J Geophys Res* **112**(D03301), doi:10.1029/2006JD007293.

Massman, W. J.: 2000, 'A simple method for estimating frequency response corrections for eddy covariance systems'. *Ag Forest Meteorol* **104**, 185–198.

Massman, W. J. and R. Clement: 2004, 'Uncertainty in eddy covariance flux estimates resulting from spectral attenuation'. In: X. Lee, W. J. Massman, and B. Law (eds.): *Handbook of micrometeorology: a guide for surface flux measurement and analysis*. Kluwer Academic Publishers, pp. 67–99.

McGillis, W. R., J. B. Edson, J. E. Hare, and C. W. Fairall: 2001a, 'Direct covariance air-sea CO_2 fluxes'. *J Geophys Res* **106**, 16,729–16,745.

McGillis, W. R., J. B. Edson, J. D. Ware, J. W. H. Dacey, J. E. Hare, C. W. Fairall, and R. Wanninkhof: 2001b, 'Carbon dioxide flux techniques performed during GasEx-98'. *Marine Chem* **75**, 267–280.

McGillis, W. R., J. B. Edson, C. J. Zappa, J. D. Ware, S. P. McKenna, E. A. Terray, J. E. Hare, C. W. Fairall, W. Drennan, M. Donelan, M. D. DeGrandpre, R. Wanninkhof, and R. A. Feely: 2004, 'Air-sea CO_2 exchange in the equatorial Pacific'. *J Geophys Res* **109**(C08S02), doi:10.1029/2003JC002256.

Miller, S., C. Marandino, W. de Bruyn, and E. S. Saltzman: 2009, 'Air-sea exchange of CO_2 and DMS in the North Atlantic by eddy covariance'. *Geophys Res Lett* **36**(L15816), doi:10.1029/2009GL038907.

Miller, S. D., C. Marandino, and E. S. Saltzman: 2010, 'Ship-based measurement of air-sea CO_2 exchange by eddy covariance'. *J Geophys Res* **115**, D02304.

Moore, C. J.: 1986, 'Frequency response corrections for eddy correlation systems'. *Boundary-Layer Meteorol* **37**(1-2), 17–35.

Nakai, T., H. Iwata, and Y. Harazono: 2011, 'Importance of mixing ratio for a long-term CO_2 flux measurement with a closed-path system'. *Tellus* **63B**, 302–308.

Nightingale, P. D., G. Malin, C. S. Law, A. J. Watson, P. S. Liss, M. I. Liddicoat, J. Boutin, and R. C. Upstill-Goddard: 2000, 'In situ evaluation of air-sea gas exchange parameterizations using novel conservative and volatile tracers'. *Global Biogeochem Cycles* **14**, 373–387.

Ohtaki, E. and T. Matsui: 1982, 'Infrared device for simultaneous measurement of fluctuations of atmospheric carbon dioxide and water vapor'. *Boundary-Layer Meteorol* **24**, 109–119.

O'Keefe, A. and D. A. G. Deacon: 1988, 'Cavity ring-down optical spectrometer for absorption measurements using pulsed laser sources'. *Rev Scientific Inst* **59**(12), 2544–2551.

O'Keefe, A., J. J. Scherer, and J. B. Paul: 1999, 'CW integrated cavity output spectroscopy'. *Chem Phys Letters* **307**, 343–349.

Oncley, S. P.: 1989, 'Parameterization techniques in the atmospheric surface layer'. Ph.D. thesis, University of California, Irvine.

Peters, G., B. Fischer, and H. Munster: 2001, 'Eddy covariance measurements with closed-path optical humidity sensors: A feasible concept?'. *J Atmos Oceanic Technol* **18**, 503–514.

Prytherch, J., M. J. Yelland, R. W. Pascal, B. I. Moat, I. Skjelvan, and C. C. Neill: 2010a, 'Direct measurements of the CO_2 flux over the ocean: Development of a novel method'. *Geophys Res Lett* **37**(L03607), doi:10.1029/2009GL041482.

Prytherch, J., M. J. Yelland, R. W. Pascal, B. I. Moat, I. Skjelvan, and V. A. Srokosz: 2010b, 'Open ocean gas transfer velocity derived from long-term direct measurements of the CO_2 flux'. *Geophys Res Lett* **37**(L23607), doi:10.1029/2010GL045597.

Rella, C.: 2010, 'Accurate greenhouse gas measurements in humid gas streams using the Picarro G1301 carbon dioxide / methane / water vapor gas analyzer'. White paper, Picarro, Inc., 480 Oakmead Pkwy, Sunnyvale, CA 94085.

Sabine, C. L., R. A. Feely, N. Gruber, R. M. Key, K. Lee, J. L. Bullister, R. Wanninkhof, C. S. Wong, D. W. R. Wallace, B. Tilbrook, F. J. Millero, T.-H. Peng,

A. Kozyr, T. Ono, and A. F. Rios: 2004, 'The oceanic sink for anthropogenic CO_2'. *Science* **305**(5682), 367–371.

Sabine, C. L., S. Hankin, H. Koyuk, D. C. E. Bakker, B. Pfeil, A. Olsen, N. Metzl, A. Kozyr, A. Fassbender, A. Manke, J. Malczyk, J. Akl, S. R. Alin, R. G. J. Bellerby, A. Borges, J. Boutin, P. J. Brown, W.-J. Cai, F. P. Chavez, A. Chen, C. Cosca, R. A. Feely, M. González-Dávila, C. Goyet, N. Hardman-Mountford, C. Heinze, M. Hoppema, C. W. Hunt, D. Hydes, M. Ishii, T. Johannessen, R. M. Key, A. Körtzinger, P. Landschützer, S. K. Lauvset, N. Lefèvre, A. Lenton, A. Lourantou, L. Merlivat, T. Midorikawa, L. Mintrop, C. Miyazaki, A. Murata, A. Nakadate, Y. Nakano, S. Nakaoka, Y. Nojiri, A. M. Omar, X. A. Padin, G.-H. Park, K. Paterson, F. F. Perez, D. Pierrot, A. Poisson, A. F. Ríos, J. Salisbury, J. M. Santana-Casiano, V. V. S. S. Sarma, R. Schlitzer, B. Schneider, U. Schuster, R. Sieger, I. Skjelvan, T. Steinhoff, T. Suzuki, T. Takahashi, K. Tedesco, M. Telszewski, H. Thomas, B. Tilbrook, D. Vandemark, T. Veness, A. J. Watson, R. Weiss, C. S. Wong, and H. Yoshikawa-Inoue: 2012, 'Surface Ocean CO_2 Atlas (SOCAT) gridded data products'. *Earth Syst Sci Data Discuss* **5**, 781–804.

Spirig, C., A. Neftel, C. Ammann, J. Dommen, W. Grabmer, A. Thielmann, A. Schaub, J. Beauchamp, A. Wisthaler, and A. Hansel: 2005, 'Eddy covariance flux measurements of biogenic VOCs during ECHO 2003 using proton transfer reaction mass spectrometry'. *Atmos Chem Phys* **5**, 465–481.

Sweeney, C., E. Gloor, A. R. Jacobson, R. M. Key, G. McKinley, J. L. Sarmiento, and R. Wanninkhof: 2007, 'Constraining global air-sea gas exchange for CO_2 with recent bomb ^{14}C measurements'. *Global Biogeochem Cycles* **21**(GB2015), doi:10.1029/2006GB002784.

Takahashi, T., S. C. Sutherland, C. Sweeney, A. Poisson, N. Metzl, B. Tilbrook, N. Bates, R. Wanninkhof, R. A. Feely, C. Sabine, J. Olafsson, and Y. Nojiri: 2002, 'Global sea-air CO_2 flux based on climatological surface ocean pCO_2, and seasnoal biological and temperature effects'. *Deep-Sea Res II* **49**, 1601–1622.

Takahashi, T., S. C. Sutherland, R. Wanninkhof, C. Sweeney, R. A. Feely, D. W. Chipman, B. Hales, G. Friederich, F. Chavez, C. Sabine, A. Watson, D. C. E. Bakker, U. Schuster, N. Metzl, H. Yoshikawa-Inoue, M. Ishii, T. Midorikawa, Y. Nojiri, A. Kortzinger, T. Steinhoff, M. Hoppema, J. Olafsson, T. S. Arnarson, B. Tilbrook, T. Johannessen, A. Olsen, R. Bellerby, C. S. Wong, B. Delille, N. R. Bates, and H. J. W. de Baar: 2009, 'Climatological mean and decadal change in surface ocean pCO_2, and net sea-air CO_2 flux over the global oceans'. *Deep-Sea Res II* **56**, 554–577.

Wanninkhof, R.: 1992, 'Relationship between wind speed and gas exchange over the ocean'. *J Geophys Res* **97**(C5), 7373–7382.

Wanninkhof, R. and W. R. McGillis: 1999, 'A cubic relationship between air-sea CO_2 exchange and wind speed'. *Geophys Res Lett* **26**(13), 1889–1892.

Webb, E. K., G. I. Pearman, and R. Leuning: 1980, 'Correction of flux measurements for density effects due to heat and water vapour transfer'. *Q J Royal Met Soc* **106**, 85–100.

Weiss, A., J. Kuss, G. Peters, and B. Schneider: 2007, 'Evaluating transfer velocity-wind speed relationship using long-term series of direct eddy correlation CO_2 flux measurements'. *J Marine Sys* **66**, 130–139.

Zhang, J., X. Lee, G. Song, and S. Han: 2011, 'Pressure correction to the long-term measurement of carbon dioxide flux'. *Ag Forest Meteorol* **151**, 70–77.